

AD-771 372

PREDICTING SOUND PHASE AND AMPLITUDE  
FLUCTUATIONS DUE TO MICROSTRUCTURE  
IN THE UPPER OCEAN

Herman Medwin

Naval Postgraduate School  
Monterey, California

15 November 1973

DISTRIBUTED BY:

**NTIS**

National Technical Information Service  
U. S. DEPARTMENT OF COMMERCE  
5285 Port Royal Road, Springfield Va. 22151

Unclassified

SECURITY CLASSIFICATION OF THIS PAGE (When Data Entered)

AD 771372

| REPORT DOCUMENTATION PAGE   |                       | READ INSTRUCTIONS<br>BEFORE COMPLETING FORM  |
|---|-----------------------|--|
| 1. REPORT NUMBER<br>NPS 61Md73111A  | 2. GOVT ACCESSION NO. | 3. RECIPIENT'S CATALOG NUMBER  |
| 4. TITLE (and Subtitle)<br>Predicting Sound Phase and Amplitude Fluctuations<br>Due to Microstructure in the Upper Ocean  |                       | 5. TYPE OF REPORT & PERIOD COVERED<br>Annual<br>1 July 72 - 25 Nov 73                              |
| 7. AUTHOR(s)<br>Herman Medwin   |                       | 6. PERFORMING ORG. REPORT NUMBER   |
| 9. PERFORMING ORGANIZATION NAME AND ADDRESS<br>Naval Postgraduate School<br>Department of Physics<br>Monterey, California 93940   |                       | 8. CONTRACT OR GRANT NUMBER(s)   |
| 11. CONTROLLING OFFICE NAME AND ADDRESS<br>Naval Ship Systems Command (PMS-302-44)<br>Department of the Navy<br>Washington, D. C. 20360   |                       | 10. PROGRAM ELEMENT, PROJECT, TASK<br>AREA & WORK UNIT NUMBERS<br>62755N(b); 12877-01<br>WR-4-7002 |
| 14. MONITORING AGENCY NAME & ADDRESS (if different from Controlling Office)   |                       | 12. REPORT DATE<br>15 November 1973  |
|   |                       | 13. NUMBER OF PAGES<br>47  |
|   |                       | 15. SECURITY CLASS. (of this report)<br>Unclassified   |
|   |                       | 15a. DECLASSIFICATION/DOWNGRADING<br>SCHEDULE  |
| 16. DISTRIBUTION STATEMENT (of this Report)<br>Approved for public release; distribution unlimited.   |                       |  |
| 17. DISTRIBUTION STATEMENT (of the abstract entered in Block 20, if different from Report)  |                       |  |
| 18. SUPPLEMENTARY NOTES<br>Research support: U. S. Naval Ship Systems Command, Code 302-44  |                       |  |
| 19. KEY WORDS (Continue on reverse side if necessary and identify by block number)<br>Sound Fluctuations<br>Ocean Microstructure<br>Upper Ocean   |                       |  |
| 20. ABSTRACT (Continue on reverse side if necessary and identify by block number)<br>The temporal and spatial variations of the index of refraction cause fluctuations of sound phase and amplitude that can be completely understood only by defining the index in terms of the duration, location, range and time of the acoustic experiment. A truncated "universal" spatial correlation function of the index has been derived from a simplified form of the Kolmogorov-Batchelor spectrum of temperature fluctuations in a homogeneous, isotropic medium. Although this correlation function is shown to be predictable simply from the depth of the |                       |  |

DD FORM 1473  
1 JAN 73  
(Page 1)EDITION OF 1 NOV 68 IS OBSOLETE  
S/N 0102-014-66011Reproduced by  
NATIONAL TECHNICAL  
INFORMATION SERVICE  
U S Department of Commerce  
Springfield VA 22151

Unclassified

SECURITY CLASSIFICATION OF THIS PAGE (When Data Entered)

20.

experiment, it is of only limited validity with respect to large spatial lags. However, a Gaussian extrapolation of the "universal" correlation function together with the standard deviation of the index provides simple useful predictions of the sound fluctuations due to temperature microstructure in the upper ocean.

NAVAL POSTGRADUATE SCHOOL  
Monterey, California

Rear Admiral M. B. Freeman  
Superintendent

M. U. Clauser  
Provost

TITLE: Predicting Sound Phase and Amplitude Fluctuations Due to Micro-  
structure in the Upper Ocean

AUTHOR: H. Medwin

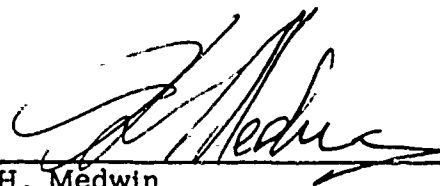
ABSTRACT:

The temporal and spatial variations of the index of refraction cause fluctuations of sound phase and amplitude that can be completely understood only by defining the index in terms of the duration, location, range and time of the acoustic experiment. A truncated "universal" spatial correlation function of the index has been derived from a simplified form of the Kolmogorov-Batchelor spectrum of temperature fluctuations in a homogeneous, isotropic medium. Although this correlation function is shown to be predictable simply from the depth of the experiment, it is of only limited validity with respect to large spatial lags. However, a Gaussian extrapolation of the "universal" correlation function together with the standard deviation of the index provides simple useful predictions of the sound fluctuations due to temperature microstructure in the upper ocean.

This task was supported by Naval Ship Systems Command (Code PMS 302).

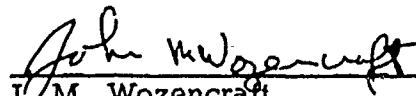


O. Heinz  
Chairman, Department of  
Physics and Chemistry



H. Medwin  
Professor of Physics  
Principal Investigator

Released by



J. M. Wozencraft  
Dean of Research

NPS-61Md73111A  
15 Nov 1973

## TABLE OF CONTENTS

1. Introduction: Sources of Sound Phase and Amplitude Fluctuations
  - 1.1 Microstructure in Mixed Water
  - 1.2 Layered Microstructure
  - 1.3 Other Underwater Structural Features
2. Wave Number Spectrum and Spatial Correlation of the Index of Refraction in a Mixed Layer
  - 2.1 The Wave Number Spectrum
  - 2.2 The Spatial Correlation and Structure Functions of the Microstructure
3. Sound Phase and Amplitude Fluctuations Due to Microstructure
  - 3.1 Phase Fluctuations
  - 3.2 Amplitude Fluctuation
  - 3.3 Small Amplitude Fluctuations: Laboratory Experiments
  - 3.4 Large Amplitude Fluctuations
  - 3.5 Fluctuations at Sea
  - 3.6 The Limits of Predictions

## 4. Conclusion

References

Initial Distribution List

Form DD 1473

## 1. Introduction

### Sources of Sound Phase and Amplitude Fluctuations

As it proceeds away from its source, a sound at sea encounters changing values of temperature, salinity and density, as well as entrained objects and bubbles in motion. These acoustically significant quantities are constant neither in space nor in time. Slower than the microscale fluctuations due to surface waves and turbulence of the medium, which show perceptible changes during a time scale of the order of seconds, are changes due to internal waves with periodicities of the order of minutes, tidal and diurnal variations, and seasonal changes. Depending on the duration of the study, some of these fluctuations may appear to be simply periodic, some show the spectral characteristics of a narrow band noise, many are describable only by statistical methods, and still others, such as the appearance of schools of fish or the incidence of storms, are largely intermittent in character. (Weston 1969). It is important to make the point that it is not the inhomogeneities but rather it is the temporal change in the position or character of the inhomogeneities that is the source of interest in this report.

The phase of a sound wave travelling through a stationary medium depends on the speed of sound along the path. This dependence is expressed by equations 1.1 and 1.2:

$$\phi = \int k \, ds = \int \frac{\omega}{c \mp |\vec{v}|} \, ds \quad (1.1)$$

where  $\phi$  = sound phase  
 $c = c(T, S, H, n(a)da)$  (1.2)

$|\vec{v}|$  = magnitude of component of material  
velocity along the ray path

$k$  = wave number along ray path

$T$  = temperature

$S$  = salinity

$H$  = depth

$n(a)da$  = number of bubbles of radius,  $a$ , in increment,  $da$

The change of amplitude of a non-divergent, unattenuated sound beam along a fixed path through the water is caused by the lens-like patches or layers in the medium which create convergences or divergences of sound power. This focusing and defocusing changes with movement of the patches, and the sound amplitude at the receiver thereby fluctuates.

### 1.1 Microstructure in Mixed Water

It will be many years before the turbulent, patchy, nature of the ocean will be unscrambled by fluid dynamicists and physical oceanographers. However, a few general concepts and landmark ideas of turbulence theory will be helpful in guiding our thinking particularly about the upper ocean.

Near the ocean surface, depending on the time of day and the meteorological history at the location, there is often a well-mixed layer of so-called "isothermal" water. The name is a reflection of the fact that common bathythermographs (BTs), show such a region as isothermal. In fact, temperature probes of higher resolution and shorter time constants have revealed that the crudely isothermal region is characterized by drifting patches of water of slightly differing temperature, Fig. 1.

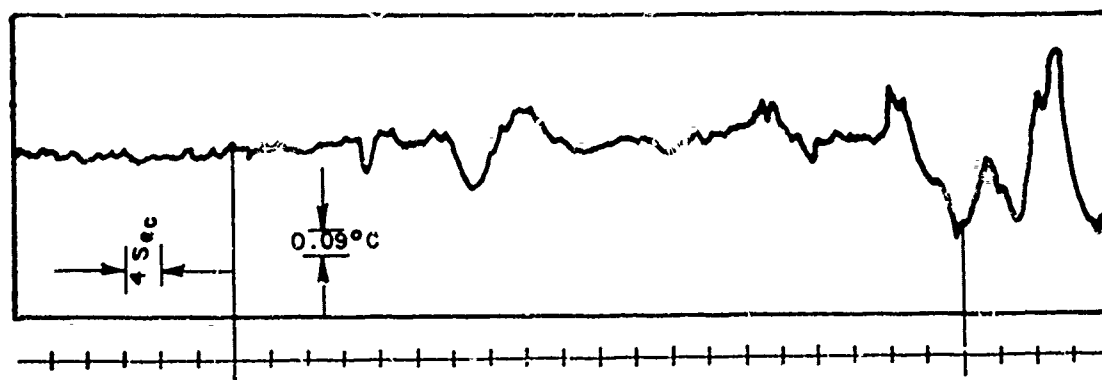


Fig. 1 Temperature fluctuations Run 6, 4.3 Meters, 0354, 22 October 1971

Within such a region there are temperature fluctuations at a point whose standard deviation,  $\sigma_T$ , may be of the order of  $0.1^\circ\text{C}$ . We will assume that this value of  $\sigma_T$  may be obtained at a point by averaging over an appropriate time, or at a given time by averaging over an appropriate local space (ergodicity). These values are a function of time of day and depth of measurement. The short-time standard deviation of the temperature fluctuations measured with respect to the mean temperature is generally greatest near the surface, greatest during the late afternoon, particularly during sunny periods. (Sagar 1960)

For example, measurements (Seymour 1971) made during the late afternoon of a sunny day in October, one mile off San Diego, Calif. reveal a decrease in  $\sigma_T$  from 0.15 to 0.14 to  $0.13^\circ\text{C}$  as the measurement depth was increased from 7 to 9 to 14 meters. The effect of night time cooling is interesting; by early morning of the following day the rms temperature fluctuations in the experiment had decreased to approximately  $0.06^\circ\text{C}$  and showed no clear dependence on depth. The water temperature gradient was only about  $0.1^\circ\text{C}/\text{meter}$ , being warmer at the surface.

Although material velocity variations generally have a lesser acoustic effect than temperature variations (Neubert 1970), there are circumstances

where the motion of the medium is significant, and may even overwhelm the temperature influence. Two situations should be considered: Near the surface of the ocean the underwater material velocity will be almost totally dependent on the surface wave height. For long-crested (swell) waves in deep water the vertical and horizontal, waveward, components of the material velocity for any frequency component of the surface wave will be almost totally orbital "near" the surface.

The depth dependence is given by

$$V(x_w, Z) = V(x_w) e^{-x_w Z} \quad (1.3)$$

where  $x_w = 2\pi/\lambda_w$  = surface wave propagation constant or  
wave number  
 $Z$  = depth

$V(x_w)$  = orbital velocity of the  $x$  wave component at the  
surface

Let us call the above underwater motion that is completely, and directly, ascribable to the surface wave action, the "coherent component" of the material velocity. Superimposed on the coherent motion of the medium there will be the "incoherent" turbulent motion, often, and for simplicity, assumed to be independent of direction. The region in which three dimensionally isotropic, or two dimensional horizontally isotropic, turbulence can be assumed to exist is a function of depth and of sea surface wave conditions. As a second example there is evidence (Dunn 1965) of horizontally isotropic turbulence in Menai Straits, 30 minutes before high tide, during low sea states at depths of 10 feet and below. The material velocity was not isotropic at 5 ft. depth.

Since the temperature fluctuations in the microstructure at sea are generally very small compared to the average temperature it is appropriate to use the linearized form of the speed dependence on temperature.

$$c = c_r + b \Delta T$$

$$\Delta c = b(T) \Delta T$$

$$\text{where } c_r = \text{reference speed at temperature, } T \quad (1.4)$$

$$\Delta c = c - c_r \quad (1.5)$$

$$b(T) = \frac{\Delta c}{\Delta T} = \text{linear rate of change of speed with temperature at } T$$



## 1.2 Layered Microstructure

It is now recognized (Woods 1966) that there are large regions of the ocean within and below the thermocline, which, for extended periods of time, possess an ordered structure of alternate layers of turbulent and relatively stable water. About one half of the ocean's regions below the mixed upper layer may show this very extensive active layered character. The active regions contain identifiable "layers", warmer than the liquid above or below them, ranging from thickness sometimes as little as 10 cm or less and extending for hundreds of meters, up to layers of thickness 10 to 15 meters extending for tens of kilometers. The layers are separated by thin "sheets" of relatively steeper temperature gradients of order  $0.01\text{ }^{\circ}\text{C}/\text{cm}$ . Temperature inversions of the same steepness with compensating salinity variations are found in these active regions. And scattered throughout the active volume there are intermittent and patchy regions, again, larger in extent than in thickness. It appears that (Nasmyth 1970) turbulence microstructure in these layers is always accompanied by temperature microstructure. On the other hand temperature microstructure has been found that it is virtually free of turbulence microstructure, and that may represent evidence of a former turbulent microstructure.

## 1.3 Other Underwater Structure Features

Frontal regions of moving water masses have been found, paralleling the meteorologist's well-developed picture of air mass behavior. For example, one might expect (Nasmyth 1970) a front with an angle of advance of  $1.5^{\circ}$ , in which quiescent warm water is being uplifted by a mass of highly turbulent colder lower water. It is not yet clear how common such situations are in the oceans of the world.

Internal waves, generated within the ocean mass, are the analogue of ocean surface waves. They are volume gravity waves which possess their maximum vertical displacement amplitude at the interface between two water masses of different densities, but their motion is detectable far above and below this interface. All the characteristics of the water mass will change at a point through which internal waves pass. For example, temperature fluctuations of a few degrees with periodicities of the order of minutes or hours are commonly found.

## 2. Spectrum and Spatial Correlation of the Index of Refraction

Studies of temperature and velocity structure within the ocean concentrate on the wave number spectral description or its transform, the spatial correlation. It is clear that patchiness of salt concentrations or bubble content at sea could also be described effectively in these same terms. The goal in turbulence research has been to find a universal spectrum.

## 2.1 The Wave Number Spectrum

The underwater material velocity that is uncorrelated with the ocean surface displacement, the turbulent velocity, cannot be completely isotropic. It is easy to see that the very long wave lengths of the Z component, at least, would be affected by the depth of the water and the depth of the mixed layer. Nevertheless, it is convenient for the theorist to talk of localized isotropic turbulence as an idealized situation.

The guiding light in turbulence studies has been the Kolmogorov Hypothesis which deals with isotropic turbulence. The Hypothesis states that, regardless of the mean flow and large scale motions (long wave length) from which turbulent energy comes, the small scale components of a "fully developed" turbulent region are in statistical equilibrium with each other. This statistical equilibrium means that the turbulent motion in a given wave length receives its time-independent energy density from larger motions and discharges it to smaller scale motions. The general behavior can be observed qualitatively in many diverse turbulent flow phenomena. Consider as examples, the smoke from the end of a cigaret or the motion of the Gulf stream. In both cases the large scale eddies break up into smaller ones and these, in turn, disintegrate into still smaller motions. If energy continues to flow at a constant rate from the largest eddies, and to be dissipated at the same rate in the smallest eddies, the intermediate scale motions contain their fixed energy densities. Ultimately the energy reaches an extremely small scale, from which it deteriorates by shear viscous losses into the random molecular motion which we identify as heat.

The band of turbulent velocity wave lengths through which the isotropic energy "cascades" from large scale to the smallest scale is called the "inertial sub-range". The smallest scale wave lengths within which viscous dissipation occurs is called the "dissipation" or "viscous sub-range". Kolmogorov assumes that, within the inertial sub-range, the turbulence is statistically independent of the large scale sources from which it originally derived. In this inertial sub-range the turbulent power spectral density,  $\Phi_v(\kappa)$  has been shown to be (Batchelor 1956) uniquely defined by the two parameters, the kinematic shear viscosity,  $\nu$ , and the rate of supply (or removal) of energy,  $\epsilon$ . The equation for the one dimensional PSD is

$$\Phi_v(\kappa) = b \kappa^{-5/3} \quad (2.1)$$

where  $b = b(\nu, \epsilon)$

$\kappa = 2\pi/\Lambda =$  wave number of a turbulent velocity component

$\Lambda =$  effective wave length of a turbulent velocity component

$\epsilon =$  energy dissipation, per unit mass, per unit time

$\nu =$  kinematic shear viscosity of water

The  $-5/3$  rds power law has been amply verified for components of turbulent velocity in laboratory experiments and, to a lesser extent, at sea.

We are interested in the turbulent velocity not only because it is a significant source of sound fluctuations in special situations such as turbulent channels but, more importantly, because it is a guide to the behavior of temperature variations. And temperature variations are generally the principal sources of sound fluctuations in the ocean.

The temperature often acts as a convected, passive contaminant which closely follows the turbulent velocity behavior. The spectrum of temperature fluctuations has been studied for such a case (Batchelor 1959) and again the  $-5/3$  law is predicted for the inertial subrange. The predictions have been largely verified (Stewart 1962, Grant 1968) by ocean measurements.

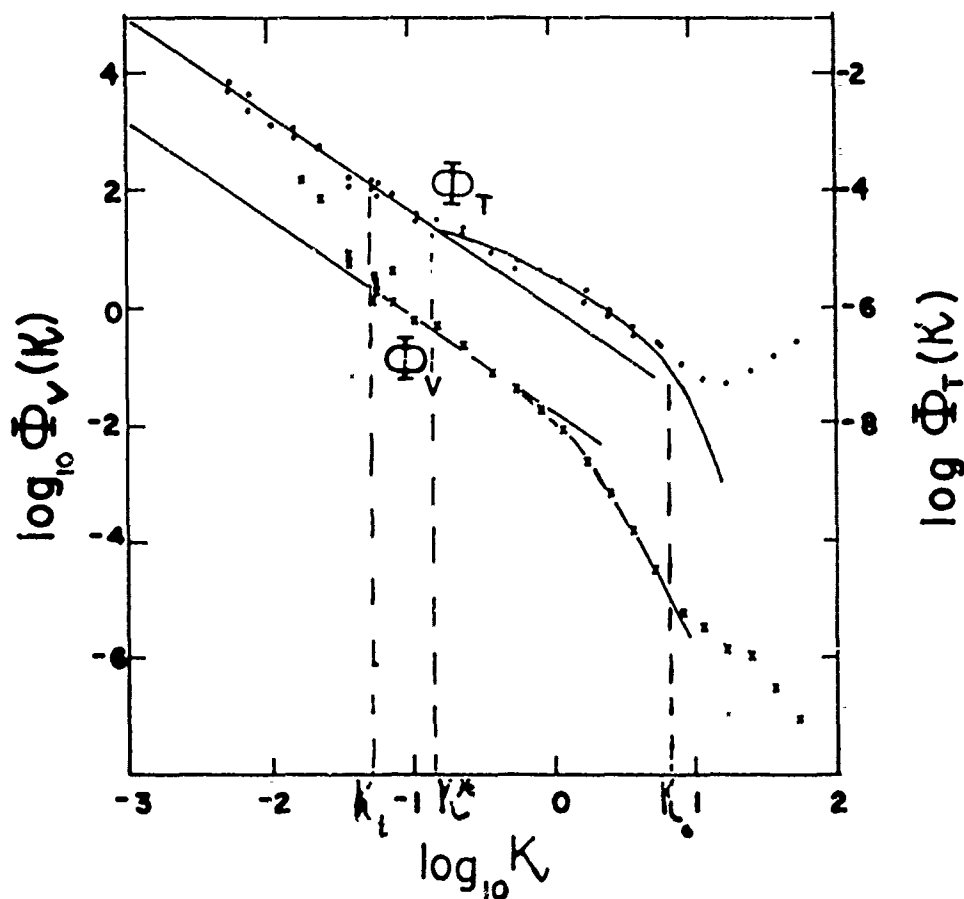


Fig. 2 Temperature and velocity spectra at depth 27m in the open sea, from Grant (1968a). The predicted transition wave number,  $\kappa_t$ , is shown, as calculated from Eq. (2.8).

Fig. 2 plots the spectra (Grant 1968) of a component of velocity and temperature measured at 27m depth, compared with the theories described in the references. The figure shows the extension of the Kolmogorov theory from the inertial subrange, where the  $-5/3$  slope is confirmed, into the higher wave number dissipation sub-range. The boundary between the two subranges is often assumed to be at the Kolmogorov wave number,

$$\kappa = \kappa_0 = (\epsilon \lambda^3)^{1/4} \quad (2.2)$$

Values of  $\epsilon$ , derived from measurements of the turbulence spectrum, are a function of depth and have been found (Grant 1968) to be as high as  $0.5 \text{ cm}^2 \text{ sec}^{-3}$  at an ocean depth of 15 meters in well-mixed water and as small as  $1.7 \times 10^{-4} \text{ cm}^2 \text{ sec}^{-3}$  in quiet water below the mixed region at 213 meter depth.

Looking again at Fig. 2 we see a rise in the temperature spectrum, also predicted by Batchelor (1959). At this depth, 27m,  $\epsilon$  was determined to be  $5.2 \times 10^{-3} \text{ cm}^2 \text{ sec}^{-3}$ . Assuming  $\nu = 1.4 \times 10^{-2} \text{ cm}^2 \text{ sec}^{-1}$ , Eq. 2.2 yields  $\kappa_0 = 6.6 \text{ cm}^{-1}$ . The rise in the temperature spectrum occurs between  $\kappa_0$  and  $\kappa^* = 2.4 \times 10^{-2} \kappa_0$ . At greater depths, the dissipation constant and the Kolmogorov wave number are generally smaller.

Having identified the high wave number end of the isotropic  $-5/3$  spectrum, we now seek to establish the low wave number limit. Unfortunately, at the low wave number end of the spectrum of temperature microstructure, the PSD is very dependent on the local conditions and history of the water mass, and only empirical results are available to guide us.

A useful, but very crude, generalization that can provide some guidance is that the largest temperature wave length that could conceivably be isotropic at the depth  $H$  would be of extent  $4H$ . The corresponding isotropic wave number would be

$$\kappa_m = \frac{2\pi}{4H} = \frac{\pi}{2H} \quad (2.3)$$

This would suggest that for Fig. 2, where  $H = 27\text{m}$ , the lower limit of the  $-5/3$  spectrum might be at

$$\kappa_m = 5.8 \times 10^{-4} \text{ cm}^{-1} \text{ (or } \log_{10} \kappa_m = -3.2 \text{)}.$$

In fact, the data of Fig. 2 show that at values of  $\kappa$  much smaller than  $5.8 \times 10^{-4}$  (perhaps at  $\kappa \approx 0.02 \text{ cm}^{-1}$ ) both the temperature and the velocity PSD break away from the  $-5/3$  slope. This suggests that, realistically, the lower

end of the  $-5/3$  spectrum to be expected at sea is somewhere between  $\kappa_m$  and  $\kappa_0$ . We will call that transition wave number,  $\kappa_t$ .

The appropriate variable to describe sound phase and amplitude fluctuations will turn out to be the speed of sound, and so it is the spectrum of fluctuations of the speed that we must seek. The connection is direct. For simplicity we will assume that the speed depends only on the temperature. We have previously seen that the fluctuations in temperature microstructure are much less than the average temperature. The fluctuations in the speed of sound are also a very small fraction of the average value. It therefore turns out to be most useful to define not only the index of refraction of the sound speed, at position  $\vec{R}$

$$n(\vec{R}) \equiv \frac{c(\vec{R})}{\langle c(\vec{R}) \rangle} \quad (2.4)$$

but also the excess index of refraction,  $\mu(\vec{R})$ , which will be the particular parameter for all future discussions of fluctuations.

$$\mu(\vec{R}) \equiv \frac{c(\vec{R}) - \langle c(\vec{R}) \rangle}{\langle c(\vec{R}) \rangle} = n(\vec{R}) - 1 \ll 1 \quad (2.5)$$

The mean value,  $\langle \rangle$ , is to be calculated over the time of the experiment. It is essential to realize that  $\mu(\vec{R})$  is sensitive to position  $\vec{R}$ . However, for typographic convenience we will drop the notation for the explicit dependence on position so that henceforth we write  $\mu(\vec{R}) \equiv \mu$ . Further, we define

$$\langle \mu \rangle = 0 \text{ and } \sigma_\mu \equiv \langle \mu^2 \rangle^{1/2} \quad (2.6)$$

The point must also be made that if the time or duration of our averaging process is changed, the value of  $\langle \mu \rangle$  and  $\sigma_\mu$  will change. We must immediately accept that these quantities must have their temporal limits restricted. A logical criterion for the restriction is that for the present we are concerned only with locally homogeneous regions of the ocean, only for times comparable to the duration of the acoustic experiment. We will be more precise about these limitations, shortly.

Since the excess index,  $\mu$ , is proportional to the excess speed of sound, which in turn is assumed to be proportional to the excess temperature,  $\Delta T$ , a spectrum of  $\mu$  can be expected to resemble the spectrum of  $\Delta T$ . It will have an inertial subrange in which the log of the power spectral density,  $\Phi_\mu(\kappa)$  will have a slope of  $-5/3$  when plotted against  $\log \kappa$ , as in Fig. 2. That isotropic inertial subrange will have an upper limit  $\kappa^*$  and a lower limit which we will call  $\kappa_t < \kappa_m$ .

The lower bound of the isotropic inertial subrange of temperature  $\kappa_t$ , appears to be approximately a function of depth,  $H$ , alone if we define it as

$$\begin{aligned}\kappa_t &= 0.5 (\kappa_o \kappa_m)^{1/2} \\ &= 0.5 \left(\frac{\epsilon}{\nu^3}\right)^{1/8} \left(\frac{\pi}{2H}\right)^{1/2}\end{aligned}\quad (2.7)$$

Fig. 3 is a graph of  $\kappa_t$ , calculated from Grant's (1968) values of  $\epsilon$  and  $H$ , as well as those of Nasmyth (1970).

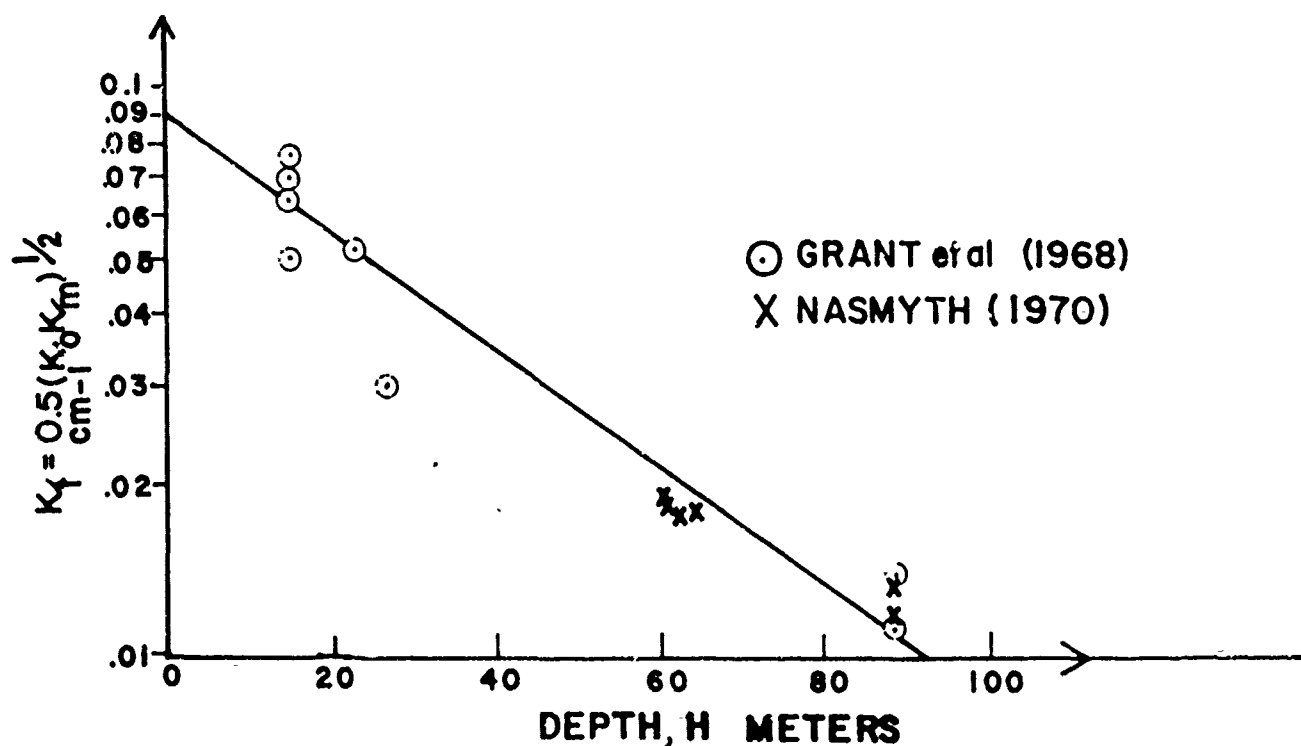


Fig. 3 Transition wave numbers, calculated from Eq. (2.7) using data of Grant (1968a) and Nasmyth (1970). The empirical fit to the data, given by Eq. (2.8) is shown.

The equation of the best simple approximation to this graph, is of the form

$$\kappa_t = B e^{-H/h} \quad (2.8)$$

where  $B = 9.0 \text{ m}^{-1}$

$h = 40.0 \text{ m}$

$H = \text{depth, m.}$

$\kappa_t = \text{lower wave number limit of isotropic temperature spectrum, m}^{-1}$

For example, for the experiment at 27M depth, shown in Fig. 2, Eq. (2.8) allows us to diagnose that the medium was no longer isotropic for  $\kappa < \kappa_t = 0.05$  ( $\log_{10} \kappa = -1.3$ ). Study of Fig. 2 verifies that especially the velocity, but also the temperature spectrum, breaks away from the  $-5/3$  slope at  $\log \kappa \approx -1.3$ . We will use the criterion of Eq. (2.8) to guide us in our prediction of acoustic fluctuations due to microstructure.

A graph of the spectrum of the expected excess index of refraction at sea is shown in Fig. 4.

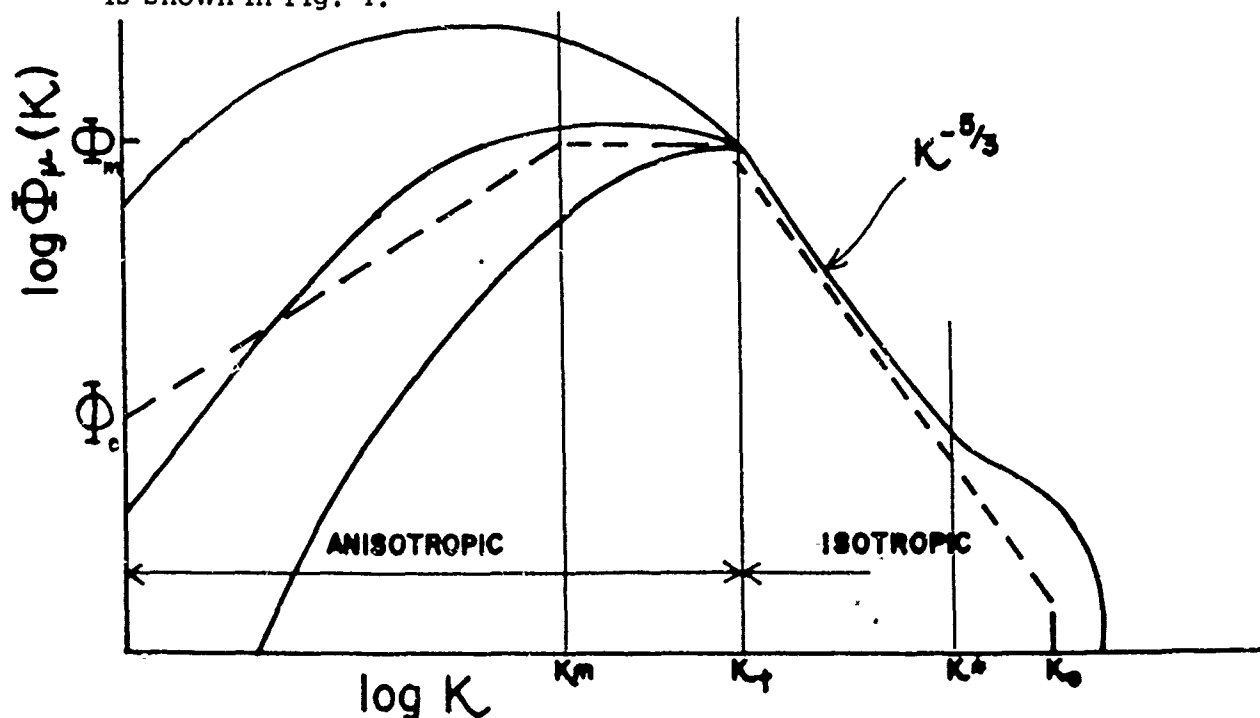


Fig. 4 Typical spectra  $\Phi_\mu(\kappa)$  and the approximate, simplified, version to be used here to calculate spatial correlation.

It is typified by: a large scale, (small wave number) non-isotropic, highly variable, section at  $\kappa < \kappa_t$  that depends on location and time of day: an isotropic universal subrange that follows the Kolmogorov Law

$$\Phi_\mu(\kappa) = b(\kappa)^{-5/3} \text{ for } \kappa_t \leq \kappa \leq \kappa^*;$$

a universal dissipation subrange with  $\Phi_\mu(\kappa) > b\kappa^{-5/3}$  for  $\kappa^* \leq \kappa \leq \kappa_0$ , and a rapid exponential drop-off for  $\kappa > \kappa_0$ . We will generalize and use this spectrum in the next section. The data available show that  $\kappa_0 \ll \kappa_t \ll \kappa_m$ .

## 2.2 The Spatial Correlation and Structure Function

The alternative to the spectral description of fluctuations of temperature or index of refraction is either the correlation function or the structure function,

which is simply derived from the spatial correlation. These functions turn out to be the most direct way to calculate the sound fluctuations, as we will see in Section 3.

One of the earliest determinations (Liebermann 1951) of the spatial correlation of temperature fluctuations was conducted by mounting a thermistor on a submarine operating at a depth of approximately 50m. The standard deviation of the temperature fluctuations was found to be approximately  $0.4^{\circ}\text{C}$  at this depth (time of day, weather conditions unreported). The spatial correlation could be fitted approximately by the exponential law (shown by solid line in Fig. 5)

$$c_T(\xi) \approx \frac{\langle T(x) T(x+\xi) \rangle}{\sigma_T^2} = e^{-\xi/a} \quad (2.9)$$

where  $a = 60\text{ cm}$

which thereby defined a correlation length, sometimes called a "patch size", of 60 cm.

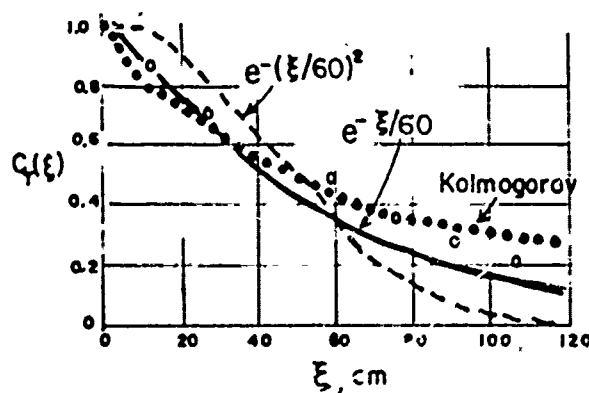


Fig. 5 Temperature correlation function from Liebermann (1951) with data (circles), empirical fits to exponential (solid line), and Gaussian (dashed line), correlation functions. The correlation based on Fig. 4 with  $\kappa_t = 0.24\text{ cm}^{-1}$  is shown by dotted line, identified as "Kolmogorov".

Others have used the Gaussian correlation function

$$C_T(\xi) = e^{-(\xi/\epsilon)^2} \quad (2.10)$$

to describe microstructure fluctuation. A Gaussian correlation function (dashed line) has been drawn in Fig. 5 for comparison with the exponential functions and the data (circles).



Both functions define the same correlation length, since they both reach  $e^{-1}$  at  $\xi = a$ . The correlation function of the index of refraction will equal that of the temperature, if other parameters affecting the speed of sound have negligible effect, and if the fluctuations are small. Then

$$C_T(\xi) = C_\mu(\xi)$$

It is not always possible to determine the correlation function  $C_T(\xi)$  or  $C_\mu(\xi)$  by measuring it directly. In any event it would be a boon if we could use the known universal characteristics of ocean microstructure to deduce the spatial correlation function in the real world outside of the laboratory. Although this turns out to be not completely feasible, there are certain generalizations about the spatial correlation function that can be deduced; one of these is its form at small values of  $\xi$ .

The spatial correlation function of the excess index of refraction can be obtained from the wave number spectrum by the Fourier transform theorem. In three dimensions this relation is

$$C_\mu(\vec{r}) = \frac{1}{\sigma_\mu^2} \iiint_{-\infty}^{\infty} S_\mu(\vec{k}) e^{i\vec{k} \cdot \vec{r}} d\vec{k} \quad (2.11)$$

where  $\vec{r}$  is the vector spatial lag.

If we now assume that the changes of the index of refraction are independent of the direction being studied we can simplify the integration. In spherical coordinates

$$\vec{k} \cdot \vec{r} = kr \cos \Theta \quad \text{and} \quad d\vec{k} = 2\pi k^2 \sin \Theta \, dk \, d\Theta$$

Then 
$$C_\mu(r) = \frac{2\pi}{\sigma_\mu^2} \int_0^\infty k^2 dk \int_0^\pi S_\mu(k) \sin \Theta e^{ikr \cos \Theta} d\Theta$$

and the  $\Theta$  integration yields

$$C_\mu(r) = \frac{4\pi}{\sigma_\mu^2} \int_0^\infty k^2 \frac{\sin kr}{kr} S_\mu(k) dk$$

We now define the one dimensional spectral function,  $\Phi_\mu(k)$  for the isotropic medium

$$S_\mu(\vec{k}) d\vec{k} = 4\pi k^2 S_\mu(k) dk = \Phi_\mu(k) dk \quad \text{and change} \quad (2.12)$$

notation,  $r \rightarrow \xi$ , for consistency with previous work, so that

$$C_{\mu}(\xi) = \frac{1}{\sigma_{\mu}^2} \int_0^{\infty} \frac{\sin \kappa \xi}{\kappa \xi} \Phi_{\mu}(\kappa) d\kappa. \quad (2.13)$$

$\xi$  may be in any assigned direction for the isotropic medium.

In order to integrate (2.13) we start with the spectral conclusions of the previous section (Fig. 4). We are prepared to make four simplifying assumptions in order to proceed:

$$\begin{aligned} 1) \quad \Phi_{\mu}(\kappa) &= \Phi_m + s(\kappa - \kappa_m) \text{ for } \kappa < \kappa_m & (2.14) \\ &\text{where } s \text{ is the slope constant} = \frac{\Phi_m - \Phi_0}{\kappa_m} & \text{Source Subrange} \\ &\Phi_m = \text{peak isotropic PSD}; \Phi_0 = \Phi(0) \\ 2) \quad \Phi_{\mu}(\kappa) &= \text{constant} = \Phi_m \text{ for } \kappa_m < \kappa < \kappa_t & \text{Transition Subrange} \\ 3) \quad \Phi_{\mu}(\kappa) &= \Phi_m (\kappa_t/\kappa)^{-5/3} \text{ for } \kappa_t < \kappa < \kappa_0 & \text{Inertial Subrange} \\ 4) \quad \Phi_{\mu}(\kappa) &= 0 \text{ for } \kappa > \kappa_0 & \text{Dissipation Subrange} \end{aligned}$$

The approximate spectrum that follows these assumptions is shown by the dashed line of Fig. 4.

The effect of the simplifying assumptions is to replace the highly variable anisotropic range and the fixed, but complicated, isotropic range by a fixed, easily-integrable, spectrum. This will permit us to assess the relative importance of each of the sub-ranges and to determine what universal generalization can be made, (if any) about  $C_{\mu}(\xi)$  at sea.

Using the assumed spectrum of Eq. (2.14) it is possible to immediately determine the excess local index of refraction,  $\sigma_{\mu}^2$ , in terms of the peak spectral density,  $\Phi_m$ , and the constants  $\kappa_m$  and  $\kappa_t$ . Recalling that the mean squared value of any fluctuating quantity may be obtained by integrating the spectral density over all values of the appropriate parameter (frequency or wave number) we find

$$\begin{aligned} \langle \mu^2 \rangle &= \int_0^{\infty} \Phi_{\mu}(\kappa) d\kappa \\ &= \Phi_m \left\{ \int_0^{\kappa_m} \left[ 1 + \frac{s}{\Phi_m} (\kappa - \kappa_m) \right] d\kappa + \int_{\kappa_m}^{\kappa_t} d\kappa + \int_{\kappa_t}^{\kappa_0} \left( \frac{\kappa_t}{\kappa} \right)^{5/3} d\kappa \right\} \end{aligned}$$

Since  $\kappa_m \ll \kappa_t$  and  $\Phi_0 < \Phi_m$ , the result of the integration simplifies to

$$\sigma_{\mu}^2 = 5/2 \kappa_t \Phi_m \quad (2.15)$$

It is interesting to determine the parts of the spectrum most responsible for this variance of the fluctuations. The terms in the integration were

|                       |                     |
|-----------------------|---------------------|
| $1/2 \kappa_m \Phi_m$ | source subrange     |
| $\kappa_t \Phi_m$     | transition subrange |
| $3/2 \kappa_t \Phi_m$ | inertial subrange   |

Since  $\kappa_m \ll \kappa_t$ , we conclude that the contributions to  $\sigma_\mu$  come almost equally from the transition and the inertial subranges. Furthermore, our simplifying assumption of the particular form of the source subrange can have little effect on  $\sigma_\mu$  because that contribution is proportional to  $\kappa_m$ , and  $\kappa_m \ll \kappa_t$ .

A second general conclusion can be reached if we restrict our interest to very small values of the spatial lag,  $\xi$ . Then we can substitute the expansion for the  $\sin \kappa \xi$  and integrate Eq. (2.13) with ease

$$\begin{aligned}
 C_\mu(\xi) &= \frac{1}{\sigma_\mu^2} \int_0^\infty \left[ \frac{\kappa \xi - (\kappa \xi)^3/3!}{\kappa \xi} \right] \Phi(\kappa) d\kappa \quad \text{for } \kappa_0 \xi \ll 1 \\
 &= \frac{1}{\sigma_\mu^2} \int_0^\infty \Phi(\kappa) d\kappa - \frac{\xi^2}{6\langle \mu^2 \rangle} \left\{ \int_{\kappa=0}^{\kappa_m} \kappa^2 [\Phi_m + m(\kappa - \kappa_m)] d\kappa \right. \\
 &\quad \left. + \int_{\kappa_m}^{\kappa_t} \kappa^2 \Phi_m d\kappa \right. \\
 &\quad \left. + \int_{\kappa_t}^{\kappa_0} \kappa^2 \Phi_m \left( \frac{\kappa_t}{\kappa} \right)^{5/3} d\kappa \right\}
 \end{aligned} \tag{2.13a}$$

The first integration yields  $\langle \mu^2 \rangle$ , as we saw above, so that the first term is unity. The integration over the three terms in the curly bracket is also simple so that

$$C_\mu(\xi) = 1 - \frac{\xi^2 \Phi_m \kappa_t^{5/3} \kappa_0^{4/3}}{8 \sigma_\mu^2} \tag{2.16}$$

and with the aid of (2.15)

$$C_\mu(\xi) = 1 - 0.05 \kappa_t^{2/3} \kappa_0^{4/3} \xi^2 \quad \text{for } \kappa_0 \xi \ll 1. \tag{2.17}$$

The significance of this result appears if we consider any specific depth, say 50m. Then (2.3) gives  $\kappa_m = \pi/10^4 \text{ cm}^{-1}$ , (2.8) predicts  $\kappa_t = 2.4 \times 10^{-2} \text{ cm}^{-1}$  and therefore, at 50m depth, we can expect

$$C_\mu(\xi) = 1 - 0.468 \xi^2$$

For small displacements this is an expansion of the Gaussian form

$$C_{\mu}(\xi) = e^{-(\xi/a)^2} \approx 1 - (\xi/a)^2; \xi \ll a$$

where  $a \approx 0.685 \text{ cm}$

We therefore conclude that at a depth of 50m the Gaussian form is appropriate only for very small spatial lags,  $\xi \ll 0.68 \text{ cm}$ . The conclusion is not significantly different at other depths.

We are now prepared to develop the universal correlation function based on the spectrum of (2.15). The correlation function will be "universal" only in so far as it is calculable from the universal part of the spectrum. To be safe, we will calculate the correlation only for  $\xi \leq \pi/\kappa_t$ .

For this restricted part of the correlation function it turns out that the universal Kolmogorov subrange is dominant so that very useful results can be obtained with a minimum of mathematical calisthenics.

Starting again with Eq. (2.13) we split the integration into the contributions for the source, transition, and inertial subranges. We have assumed zero spectral density in the dissipation subrange so that integral is zero.

$$\sigma_{\mu}^2 C_{\mu}(\xi) = \int_{\kappa=0}^{\kappa_m} \frac{\sin \kappa \xi}{\kappa \xi} [\Phi_m + s(\kappa - \kappa_m)] d\kappa + \int_{\kappa_m}^{\kappa_t} \frac{\sin \kappa \xi}{\kappa \xi} \Phi_m d\kappa + \int_{\kappa_t}^{\infty} \frac{\sin \kappa \xi}{\kappa \xi} \Phi_m \left(\frac{\kappa_t}{\kappa}\right)^{5/3} d\kappa$$

The coordinate for integration is now changed to  $\beta = \kappa \xi$

$$\sigma_{\mu}^2 C_{\mu}(\xi) = \frac{1}{\xi} \int_{\beta=0}^{\kappa_m \xi} \left[ \frac{\sin \beta}{\beta} \right] [\Phi_m + s(\frac{\beta}{\xi} - \kappa_m)] d\beta + \frac{1}{\xi} \int_{\beta=\kappa_m \xi}^{\kappa_t \xi} \left( \frac{\sin \beta}{\beta} \right) \Phi_m d\beta + \xi^{2/3} \int_{\beta=\kappa_t \xi}^{\infty} \frac{\sin \beta}{\beta} \Phi_m \left( \frac{\kappa_t \xi}{\beta} \right)^{5/3} d\beta$$

The approximations are now made for  $\int \frac{\sin \beta}{\beta} d\beta = \beta - \frac{\beta^3}{3 \cdot 3!} + \frac{\beta^5}{5 \cdot 5!}$  in the source integral and in the transition integral. Because of the rapid convergence due to the  $\beta^8/3$  in the denominator, the third integral is comfortably approximated by using the sine expansion from zero to  $\pi/2$  and again from  $\pi/2$  to  $\pi$ . Using (2.15) the result of these integrations, valid for  $\xi \leq \frac{\pi}{\kappa_t}$  with about 5% error, is

$$C_{\mu}(\xi) = 1.0 - 0.48(\kappa_t \xi)^{2/3} + 0.28(\kappa_t \xi)^2 + 6.7 \times 10^{-4}(\kappa_t \xi)^4 \quad (2.18)$$

The curve is shown in Fig. 6

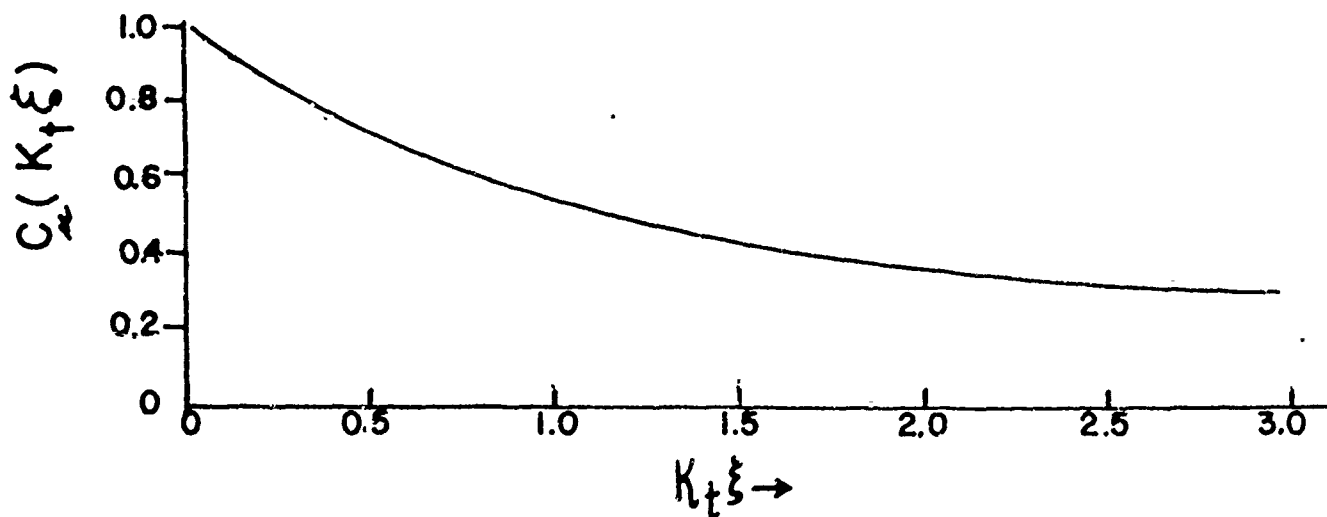


Fig. 6 Spatial correlation function  $C_{\mu}(\kappa_t \xi)$  derived from spectrum of Fig 4.

It turns out that the source subrange makes essentially no contribution to the correlation function for  $\xi \leq \pi/\kappa_t$ ; its effect would be for greater spatial lags. The transition and inertial subranges, together, are totally responsible for  $C_{\mu}(\xi)$  for  $\xi \leq \pi/\kappa_t$ . The inertial subrange is particularly dominant for small spatial lags (the  $2/3$  power term).

Assuming that  $\kappa_t$  is given by Eq. (2.8), it is possible to calculate  $C_{\mu}(\xi)$  for any depth. The calculation has been made for the depth of Liebermann's experiment (50m), for which Eq. (2.8) gives  $\kappa_t = 0.024 \text{ cm}^{-1}$ , and the predicted correlation is plotted as the dotted line in Fig. 5. The agreement with the experimental data is remarkably good, up to the limiting spatial lag,  $\xi \approx \pi/\kappa_t$ .

Recapitulating, the universal spatial correlation function that has been derived from the assumed isotropic ocean spectrum has a Gaussian correlation function from  $\xi=0$  to approximately  $\xi \approx 2\pi/\kappa_0$ . It then drops off with a slope of close to  $-2/3$  under the control of the inertial subrange. This slope decreases to close to zero at the limit of our study,  $\xi = \pi/\kappa_t$ . Experimental studies show that, beyond  $\xi = \pi/\kappa_t$  the correlation value will continue to decrease slowly, begin to oscillate about this drop-off with a spatial periodicity and a specific character that depends on the precise form of the spectrum in the transition and the source subranges.

### 3. SOUND PHASE AND AMPLITUDE FLUCTUATIONS

#### 3.1 Phase Fluctuations

Let us begin our study of the variable propagation of sound in the ocean by considering plane wave sound phase fluctuations along a ray path in a statistically homogeneous, isotropic, medium. We will assume that the sound frequency is high enough so that the wave length is much smaller than the correlation length of the microstructure, that is  $ka \gg 1$ . Again  $a$  is the correlation length, the distance in which the spatial correlation drops to  $e^{-1}$ . We will first consider the ray approximation, and relatively small propagation path, so that  $ka \gg R/a$ , where  $R$  = path length.

The dual condition is best written in terms of the wave parameter,

$$D \equiv \frac{4R}{ka^2} \quad (3.1)$$

For this ray development (Bergmann 1946) we require  $D \ll 1$ . The time to travel the distance,  $R$ , in the  $x$  direction is given by

$$t = \int_0^R \frac{dx}{c(x,T)} = \int_0^R \frac{n(x,T)}{c_0} dx$$

where  $n = c/c_0$  = local index of refraction of the medium,  $T$  = clock time and  $c_0 = \langle c \rangle$ . Both  $c$  and  $n$  are functions of position and time of the experiment.

The particular duration required for this traverse will depend on the type and arrangement of inhomogeneities at the instant of the sound travel. The time of travel is assumed to be short compared to the time for the medium to rearrange itself. That is, the medium is assumed to be "frozen" during the sound traverse, and to change into another configuration during the time between traverses.

Our interest is in the duration of the travel, averaged over either many statistically equivalent inhomogeneous paths, or averaged over many traverses along a time-varying inhomogeneous path. We assume that these two averaging processes are equivalent, that is, we assume that the medium is ergodic.

$$\langle t \rangle = \frac{1}{c_0} \int_0^R \langle n(x,T) \rangle dx = \frac{1}{c_0} \int_0^R dx$$

because the average

index,  $\langle n \rangle$ , is unity.

It is the deviation from the mean that we must calculate:

$$\begin{aligned}\Delta t &= t - \langle t \rangle = \frac{1}{c_0} \int_0^R n(x, T) dx - \frac{1}{c_0} \int_0^R dx \\ &= \frac{1}{c} \int_0^R \mu(x, T) dx\end{aligned}$$

$$\text{where } \mu(x, T) = n(x, T) - 1$$

From this we get the square of the deviation from the mean  $(\Delta t)^2 = \left(\frac{1}{c}\right)^2 \left(\int_0^R \mu dx \int_0^R \mu dx\right)$  which can be written  $(\Delta t)^2 = \frac{1}{c^2} \int_0^R \int_0^R \mu(x_1, T) \mu(x_2, T) dx_1 dx_2$

The mean square deviation from the mean is  $\langle \Delta t^2 \rangle = \frac{1}{c^2} \int_0^R dx_1 \int_0^R \langle \mu(x_1, T) \mu(x_2, T) \rangle dx_2$

The integrand can be written in terms of the spatial correlation of the excess index of refraction  $C_\mu(\xi)$ :

$$\langle \mu(x_1, T) \mu(x_2, T) \rangle = \langle \mu^2 \rangle C_\mu(x_2 - x_1) = \sigma_\mu^2 C_\mu(x_2 - x_1) \quad (3.2)$$

$$\text{In these terms } \langle \Delta t^2 \rangle = \frac{\sigma_\mu^2 R}{c^2} \int_0^R C_\mu(x_2 - x_1) dx_2 \quad (3.3)$$

We seek the mean squared phase fluctuation which is calculated by substituting  $\varphi = \omega \Delta t$  where  $\varphi$  is the instantaneous deviation of the phase from the value due to the mean speed,  $c_0$ . The units of  $\varphi$  are radians. Since the medium is presumed to be statistically homogeneous, it is the separation,  $\xi = |x_2 - x_1|$ , that is significant not the particular end points,  $x_2$  or  $x_1$ . Therefore, the mean squared phase fluctuation is

$$\langle \varphi^2 \rangle = \sigma_\mu^2 k^2 R \int_0^R C_\mu(\xi) d\xi \quad D \ll 1 \quad (3.4)$$

Since  $\langle \varphi^2 \rangle = \langle \varphi \rangle^2 + \text{Var } \varphi$  and  $\langle \varphi \rangle = 0$ , by definition,  $\langle \varphi^2 \rangle = \text{Var } \varphi = \sigma_\varphi^2$ . (3.5)

We have only to know the spatial correlation of the index of refraction, from the source to the receiver, in order to carry out the integration, and obtain the variance of  $\varphi$ .

It should be pointed out that the quantity  $\sigma_\mu^2 = \langle \mu^2 \rangle$  must be known at the time, and location of experiment. The significance of this comment is that, in the ocean, the evaluation of  $\sigma_\mu^2$  can be strongly dependent on position and the range at a given time, or a function of the time and duration of measurement.

For example during passage of an internal wave, at positions in the thermocline there will be large variations of the temperature and the speed of sound, over times of the order of several minutes.

It is also convenient, sometimes, to assume that the spatial correlation function drops to zero after a few correlation lengths in either direction from any reference point. Then for the sound path of length  $R \gg a$  we can extend the integration to infinity in both directions, or double the integration from zero to infinity, without affecting the total integration,

$$\sigma_{\varphi}^2 = \langle \varphi^2 \rangle = 2 \sigma_{\mu}^2 k^2 R \int_0^{\infty} C_{\mu}(\xi) d\xi \quad D \ll 1 \quad (3.6)$$

Given a correlation function that drops rapidly and monotonically to zero, Eq. (3.6) is more readily evaluated for the mean squared phase fluctuation for the high frequency condition than (3.4).

When the path is long, so that phase interferences occur, a wave analysis is necessary. We will not go through the derivation for the phase fluctuations through the same type of medium at this other extreme of propagation parameters, but simply quote the result (Chernov 1967), applicable for low frequencies or very large path lengths.

$$\sigma_{\varphi}^2 = \langle \varphi^2 \rangle = \sigma_{\mu}^2 k^2 R \int_0^{\infty} C_{\mu}(\xi) d\xi \quad D \gg 1 \quad (3.7)$$

The point to be observed at this time is that, regardless of the value of the wave parameter,  $D$ , the variance of the fluctuations of phase are proportional to the length of the sound path, the sound frequency squared, and the variance of the fluctuation of the excess index of refraction,  $\sigma_{\mu}^2$ , along the path. Furthermore, regardless of the form of the spatial correlation function, there is only the factor, 2, relating the mean square phase fluctuation obtained for very large or very small values of the wave parameter,  $D$ . This factor will not be altered if we change the form of the spatial correlation function, either for convenience in the evaluation of the integrals, or as we seek to describe the medium more accurately.

Another point must be made at this time. Mintzer (1954) has shown that solutions such as we are considering can be valid only for single scattering in a weakly inhomogeneous medium. That is, although we have  $ka \gg 1$  as a requirement for the relative size of the "patches", and  $kR \gg 1$  as a requirement for far field propagation, the fluctuations of the medium,  $\sigma_{\mu}^2$  must be so small that

$$k^2 \sigma_{\mu}^2 aR \ll 1$$

In practice this condition is not difficult to fulfill; field measurements generally show  $\sigma_{\mu}^2 < 10^{-8}$ .



The Gaussian correlation function

$$C(\xi) = e^{-(\xi/a)^2} \quad (3.8)$$

is attractive because of the simplicity in evaluating the integrals of Eqs. (3.6) and (3.7). For the Gaussian correlation function the phase fluctuations are:

$$\sigma_\varphi^2 = \langle \varphi^2 \rangle = \sqrt{\pi} \sigma_\mu^2 k^2 R a \quad D \ll 1 \quad (3.9)$$

$$\text{and} \quad \sigma_\varphi^2 = \langle \varphi^2 \rangle = \frac{\sqrt{\pi}}{2} \sigma_\mu^2 k^2 R a \quad D \gg 1 \quad (3.10)$$

It has been shown (Krasilnikov 1956, and Chernov 1967) that, for a Gaussian correlation function, the variance of phase fluctuations over all values of  $D$  is described by

$$\sigma_\varphi^2 = \frac{\sqrt{\pi}}{2} \sigma_\mu^2 k^2 R a \left( 1 + \frac{1}{D} \tan^{-1} D \right) \quad (3.11)$$

### 3.2 Amplitude Fluctuations

The amplitude fluctuations are often put in terms of the ratio of the change of the pressure amplitude to the original amplitude,

$$x = \left( \frac{P - P_0}{P_0} \right) \quad (3.12)$$

where  $P$  is the sound amplitude at  $x = R$  and  $P_0$  is the amplitude of the plane wave at the starting position  $x = 0$ . In terms of this parameter it turns out (Bergmann 1946, Mintzer II 1953, Chernov 1967) that the mean squared fluctuation of amplitude in the high frequency extreme is

$$\sigma_A^2 = \langle x^2 \rangle = \frac{\sigma_\mu^2}{6} R^3 \int_0^\infty \left( \frac{\partial^2}{\partial \eta^2} + \frac{\partial^2}{\partial \xi^2} \right) \left[ \frac{\partial^2 C_\mu(\xi, \eta, z)}{\partial \eta^2} + \frac{\partial^2 C_\mu(\xi, \eta, z)}{\partial \xi^2} \right] d\xi \quad (3.13)$$

for  $D = 4R/ka^2 \ll 1$

and in the wave interference region (Mintzer I 1953) it is simply

$$\sigma_A^2 = \langle x^2 \rangle = \sigma_\mu^2 k^2 R \int_0^\infty C_\mu(\xi) d\xi \quad D \gg 1 \quad (3.14)$$

where  $\sigma_A$  is the fractional standard deviation of the pressure amplitude

$$\sigma_A = \left( \left\langle \left( \frac{P - P_0}{P_0} \right)^2 \right\rangle \right)^{1/2} \quad (3.14a)$$

Comparison of expressions for amplitude fluctuations with those for phase fluctuations is revealing. For example, for the high frequency situation  $D \ll 1$  the mean squared amplitude fluctuations depend on an integration of the fourth derivative of the correlation function in the transverse directions,  $y$  and  $z$ , rather than a straightforward integration over the correlation function in the  $x$  direction as in Eq. (3.8) for the phase shift. This means that the amplitude fluctuation is caused by the curvature (really double curvature) of the correlation of the refractive index, transverse to the sound path. The dimpled medium in the case of amplitude fluctuations therefore behaves as a series of lenses converging or diverging acoustic energy along the sound path (notice the evaluation at zero displacement in the  $y$  and  $z$  direction, that is, along the beam).

At the other extreme of propagation parameters, however, when the range is larger, or the frequency is lower, such that  $R/a \gg ka$  ( $D \gg 1$ ), the sound field fluctuations are caused by field distortions due to a large number of inhomogeneities along the path in the medium; these distortions interfere, constructively and destructively along the entire path and this interference effect is common to both phase and amplitude. For this condition the mean squared fluctuations of phase and amplitude are identical. Both are linearly dependent on: a) the distance of propagation, b) the frequency squared, and c) the integrated spatial correlation function.

It must be pointed out that all of the derivations to this point have been based on the assumption of single scattering by weak fluctuations. The consequent solutions are valid only in so far that very long paths and very large fluctuations are not allowed. In practical propagation over very long paths the magnitude of the phase and amplitude fluctuations cannot increase with  $R$  without limit, or they would reach the absurd condition of fluctuations that are greater than the quantity itself. In fact, "saturation" must take place and the increase of the fluctuation with range must reach a limit that will be indicated, shortly.

If the Gaussian correlation function of the index is assumed (Krasilnikov 1956) the variance,  $\sigma_A^2$ , is:

$$\sigma_A^2 \langle \chi^2 \rangle = \left[ \frac{\sqrt{\pi}}{2} \langle \mu^2 \rangle k^2 R a \left( 1 - \frac{1}{D} \tan^{-1} D \right) \right] \quad (3.15)$$

$$\sigma_A^2 \langle \chi^2 \rangle = \left( \frac{8\sqrt{\pi}}{3} \right) \sigma_\mu^2 (R/a)^3 \quad D \ll 1 \quad (3.16)$$

$$\sigma_A^2 = \langle \chi^2 \rangle = \left( \frac{\sqrt{\pi}}{2} \right) \sigma_\mu^2 k^2 (Ra) \quad D \gg 1 \quad (3.17)$$

### 3.3 Small Amplitude Fluctuations: Laboratory Experiments

The dependence of small values of  $\sigma_A^2$  on the parameters of the medium and the frequency has been put on a firm experimental basis in a beautiful set of laboratory studies (Stone and Mintzer 1962) in which the microstructure of the index of refraction was obtained by heating the tank of water through which the sound beam was propagated. First the rms value and the spatial correlation function of the temperature microstructure were obtained by direct measurement. From these data the value  $\sigma_\mu^2$ , and the correlation function,  $C_\mu(\xi)$ , of the excess index of refraction were calculated. The spatial correlation function was fitted to the Gaussian form, and the correlation length,  $a$ , was calculated from Eq. (3.8). The measured temperature microstructure, fitted to the Gaussian correlation function showed a correlation length,  $a = 3.5$  cm.

Additional comparison showed that the rms excess index of refraction, deduced acoustically, was approximately 25% less than the value  $1.6 \times 10^{-4}$ , calculated directly from temperature measurements. One flaw was revealed in the experiment: the acoustically determined value or the assumed Gaussian correlation length was only about one-third of the value (3.5 cm) directly measured by thermistors. This discrepancy was possibly due to the error of assuming that the correlation function was Gaussian. As shown in section 2, the Gaussian form is appropriate only for very small displacements. A combination of Gaussian and Kolmogorov correlation functions would probably have been a better description of the medium for insertion into Eqs. (3.13) or (3.14).

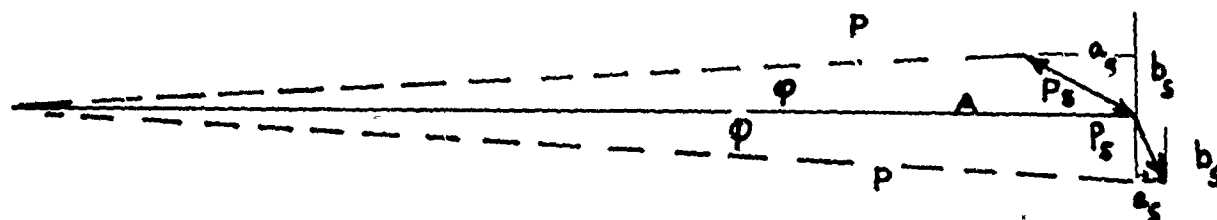
### 3.4 Large Amplitude Fluctuations - Large Ranges

So far we have considered small fluctuations for two cases:

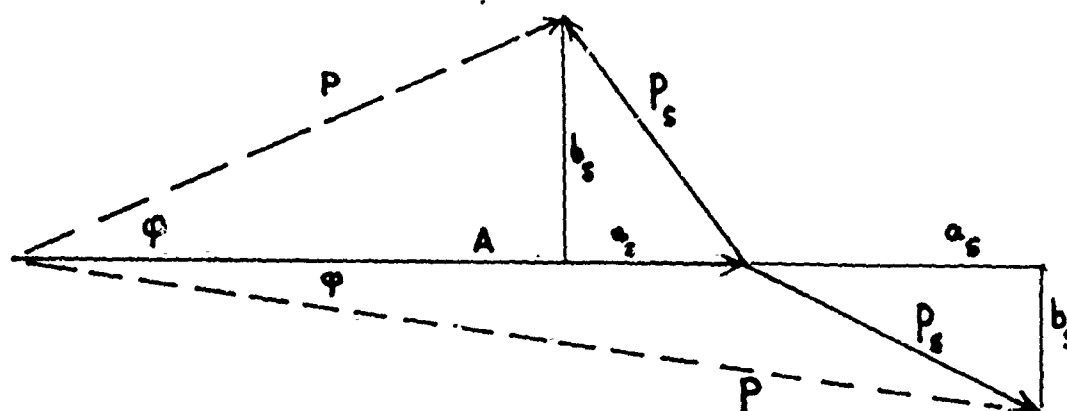
1) Change of sound pressure amplitude,  $P$ , in the presence of zero (or negligible) phase shift. In section 3.2 we gave expressions for  $\sigma_A^2 = \langle \left( \frac{P - P_0}{P_0} \right)^2 \rangle$ . The type of pressure field at  $x = R$  that results in  $\sigma_A^2$  is

described by the phase diagram for "P" in Fig 7a where  $P_s$  represents two possible scattered pressures at time,  $t$  position  $x$ . It is the vector addition of various values of  $P_s$  to the undisturbed field,  $A(x)$ , that results in the statistically changing resultant pressure amplitude,  $P$ , at angle  $\varphi$ , with the original wave. This  $P$  is used to calculate  $\sigma_A^2$ . It is to be noted that the random amplitude  $P_s$  has components,  $a_s$ , in phase with the original wave,  $A$ , and  $b_s$ ,  $90^\circ$  out-of-phase with  $A$ . It is  $a_s$  rather than  $b_s$  that is effective in changing the value of  $P$ .

2) Change of sound phase due to varying index of refraction. In the derivations of section (3.1) leading to expressions for  $\sigma^2$  it was assumed that amplitude fluctuations have a negligible effect on phase fluctuations. From Fig. 7a it is seen that the out-of-phase component of scatter  $b_s$ , rather than  $a_s$ , is the principal source of phase changes.



(a) SMALL FLUCTUATIONS



(b) LARGE FLUCTUATIONS

Fig. 7

Two realizations of scattered pressure,  $P_s$  added to undisturbed pressure  $A$ .  $P_s$  is composed of the in-phase part,  $a_s$  and the out-of-phase part,  $b_s$ . For small fluctuations Fig. 7a the pressure amplitude  $P$ , is principally a function of  $A$  and  $a_s$  only, and the phase  $\phi$  is principally determined by  $A$  and  $b_s$ . For large fluctuations Fig. 7b both  $P$  and  $\phi$  depend on  $A$ ,  $a_s$  and  $b_s$ .

We now consider large fluctuations for which the situation of Fig. 7b is more appropriate. We will no longer consider that the phase fluctuations have negligible effect on the mean square amplitude or that the amplitude fluctuations have negligible effect on the mean square phase.

The complete picture at  $x = R$ , which we have represented in Fig. 7 can be described analytically by

$$p(x, t) = A(x) \cos (\omega t - kx) + a_s (x, t) \cos (\omega t - kx) + b_s (x, t) \sin (\omega t - kx) \quad (3.18)$$

where  $A(x)$  is the magnitude of the pressure of the remaining unscattered field at  $x$ ;

$a_s(x, t)$  = time varying magnitude of the scattered pressure which is in phase with the original wave at  $x$ . We assume that values of  $a_s$  are Gaussian distributed and that  $\langle a_s \rangle = 0$ ;

$b_s(x, t)$  = time varying magnitude of the scattered pressure which is  $90^\circ$  out-of-phase with the original wave at  $x$ . We assume  $b_s$  is Gaussian distributed and  $\langle b_s \rangle = 0$ .  $b_s \leq A$ .

Equation (3.18) resolves the fluctuation scattered pressure,  $P_s$  of Fig. 7 into components in-phase with the depleted original wave  $A(x)$  and out-of-phase with it. A typical situation in Fig. 7 shows that

$$P_s^2 = a_s^2 + b_s^2$$

To get the typical amplitude,  $P$ , of the total wave at  $x$  as a function of  $A$ ,  $a_s$ ,  $b_s$ , Eq. (3.18) is rearranged to

$$P = (A + a_s) \cos(\omega t - kx) + b_s \sin(\omega t - kx) \quad (3.19)$$

$$= \underline{P} \cos(\omega t - kx - \Phi)$$

$$\text{where } \underline{P} = \text{pressure amplitude at } x \quad (3.20)$$

$$= [(A + a_s)^2 + b_s^2]^{1/2}$$

$$\Phi = \text{phase angle with respect to original}$$

$$\text{wave at } x = \tan^{-1} \left( \frac{b_s}{A + a_s} \right) \quad (3.21)$$

It is useful to expand  $\underline{P}$  and  $\Phi$  for small fluctuations  $a_s \approx b_s \ll A$ . Using the binomial theorem for  $\underline{P}$

$$\begin{aligned} \underline{P} &= A \left( 1 + \frac{2a_s}{A} + \frac{a_s^2 + b_s^2}{A^2} \right)^{1/2} \\ &\approx A \left( 1 + \frac{a_s}{A} + \frac{a_s^2 + b_s^2}{2A^2} \right) \approx A + a_s \end{aligned} \quad (3.22)$$

and the small angle approximation for  $\Phi$

$$\Phi = \tan^{-1} \left( \frac{b_s}{A + a_s} \right) \approx \frac{b_s}{A} \quad (3.23)$$

It is therefore clear that for small fluctuations the  $\sigma_A^2$  of Eq. (3.12) and (3.17) can be interpreted from the point of view of (3.18) and (3.22)

$$\chi = \frac{p-p_0}{p_0} \approx \frac{A + a_s - A_0}{A_0}$$

$$\text{so that } \sigma_A^2 = \text{Var}(\chi) = \frac{\text{Var } a_s}{A_0^2} \quad (3.24)$$

As we anticipated from our study of Fig. 7a, the value of  $\sigma_A^2$  is therefore relatively independent of the out-of-phase components of scatter,  $b_s$ , because their effect shows up to be relatively small in the small fluctuation approximation of (3.22).

Likewise, for phase fluctuations the  $\sigma_\phi^2$  of Eq. (3.4) - (3.11) can be understood from (3.18) and (3.23) as

$$\sigma_\phi^2 = \frac{\text{Var } b_s}{A^2} \quad (3.25)$$

which shows that the value of  $\sigma^2$  is virtually independent of the in-phase variations,  $a_s$ , in the small fluctuation approximation of (3.23).

For large fluctuations we follow the method of Brownlee (1973). First we recognize that the diversion of acoustical energy into scattered energy will cause the average in-phase pressure amplitude to reduce from the value  $A_0$  at  $x=0$  to  $A$  at  $x$ ; we will assume that the rate of attenuation from the original magnitude is proportional to the distance traveled,

$$\frac{dA}{A} = -\alpha_s dx$$

where  $\alpha_s$  = attenuation of the original wave due to scattered energy.

Integrating for a range  $L$ ,  $A = A_0 e^{-\alpha_s R}$  where  $A_0 \equiv P_0$  = pressure amplitude of (unscattered) wave at  $x=0$ . (3.26)

The average intensity of the part of the wave in step with the original wave will therefore be proportional to

$$A^2 = A_0^2 e^{-2\alpha_s R} \quad (3.27)$$

We will assume conservation of energy for the total wave system; that is, we assume that whatever energy is taken from the original wave goes into the scattered wave and that this is principally forward scattered (Skudrzyk 1961). This means that the intensity is conserved, when averaged over any plane perpendicular to the direction of propagation.

From (3.20)

$$\begin{aligned}
 \langle p_o^2 \rangle &= \langle p^2 \rangle \\
 \langle A_o^2 \rangle &= \langle (A+a_s)^2 + b_s^2 \rangle \\
 &= \langle A^2 \rangle + \langle 2a_s A \rangle + \langle a_s^2 \rangle + \langle b_s^2 \rangle \\
 A_o^2 &= A^2 + \langle a_s^2 \rangle + \langle b_s^2 \rangle
 \end{aligned} \tag{3.28}$$

To determine the attenuation rate,  $\alpha_s$ , we use (3.27) and (3.28) and form

$$\frac{A_o^2 - A^2}{A_o^2} = - \frac{\langle a_s^2 \rangle + \langle b_s^2 \rangle}{A_o^2} = 1 - e^{-2\alpha_s R} \tag{3.29}$$

The evaluation can be made in the small fluctuation range where the ingredients of (3.29) are well known. There, using the expansion of the exponential for small argument and (3.24) and (3.25)

$$\sigma_A^2 + \sigma_\varphi^2 = 2\alpha_s R \tag{3.30}$$

The condition for long range is of particular interest.

Then we have, from (3.7) and (3.14)

$$\sigma_A^2 = \sigma_\varphi^2, D \gg 1 \tag{3.31}$$

so that the attenuation constant of the original beam due to energy going into fluctuations, is

$$\alpha_s = \sigma_A^2 / R, D \gg 1 \tag{3.32}$$

In particular, when the scatter is due to a medium with a Gaussian correlation function,  $C_\mu(\xi)$ , we have, using (3.17),

$$\alpha_s = \frac{\sqrt{\pi}}{2} \sigma_\mu^2 K^2 a \tag{3.33}$$

We can now proceed to consider large ranges and large fluctuations. The quantity observed in any experiment is the pressure amplitude  $P$ . Eq. (3.20) shows  $P$  to be a function of all three quantities: The steady coherent component,  $A$ , and the fluctuating random components,  $a_s$  and  $b_s$ . The conventional way to express the amplitude variations is in the ratio

$$(\text{CAV})^2 = \frac{\langle P^2 \rangle - \langle P \rangle^2}{\langle P \rangle^2} \quad (3.34)$$

where  $\text{CAV}$  = coefficient of amplitude fluctuations. It might be noted that for small fluctuations we have simply  $\text{CAV} = \sigma_A$ , Eq. (3.14a). Here, for large fluctuations we find, from the conservation of energy assumption that

$$\langle P^2 \rangle = \langle P_0^2 \rangle = A_0^2 \quad (3.35)$$

But the calculation of  $\langle P \rangle^2$  involves a more involved evaluation of the mean value of  $P$  given by Eq. (3.20) when both  $a_s$  and  $b_s$  vary randomly, each with an assumed Gaussian probability density function.

The mean value of the sum has been found by Brownlee (1973) and is

$$\begin{aligned} \langle P \rangle &= \frac{\sqrt{\pi}}{2} A_0 \{1 - e^{-2\alpha_s R}\}^{\frac{1}{2}} \{ \exp[-2/(e^{2\alpha_s R} - 1)] \}^{\frac{1}{2}} \Sigma \\ \text{where } \Sigma &= 1 + 3b + \frac{(3.5)b^2}{(2!)^{\frac{1}{2}}} + \frac{(3.5.7)b^3}{(3!)^{\frac{1}{2}}} + \dots \\ b &= \frac{1}{2}(e^{2\alpha_s R} - 1)^{-1} \end{aligned} \quad (3.36)$$

When this is now squared and combined with  $P^2$  in Eq. (3.34) the  $A_0^2$  cancels and the result is expressible solely in terms of the attenuation constant,  $\alpha_s$ , and the length of path,  $R$ .

$$(\text{CAV})^2 = -1 + \frac{4}{\pi} \exp\left(\frac{2}{\exp(2\alpha_s R) - 1}\right) \{[1 - \exp(-2\alpha_s R)][\Sigma^2]\}^{-1} \quad (3.37)$$

This messy expression has a simple maximum value for large fluctuation and large ranges; we get

$$\begin{aligned} (\text{CAV})^2 &= -1 + \frac{4}{\pi} = 0.273 \quad \text{for } 2\alpha_s R \gg 1 \\ \text{or } (\text{CAV})_{\text{max}} &= 0.522 \end{aligned} \quad (3.38)$$

The complete behavior of the coefficient of amplitude variation is shown in Fig. 8.



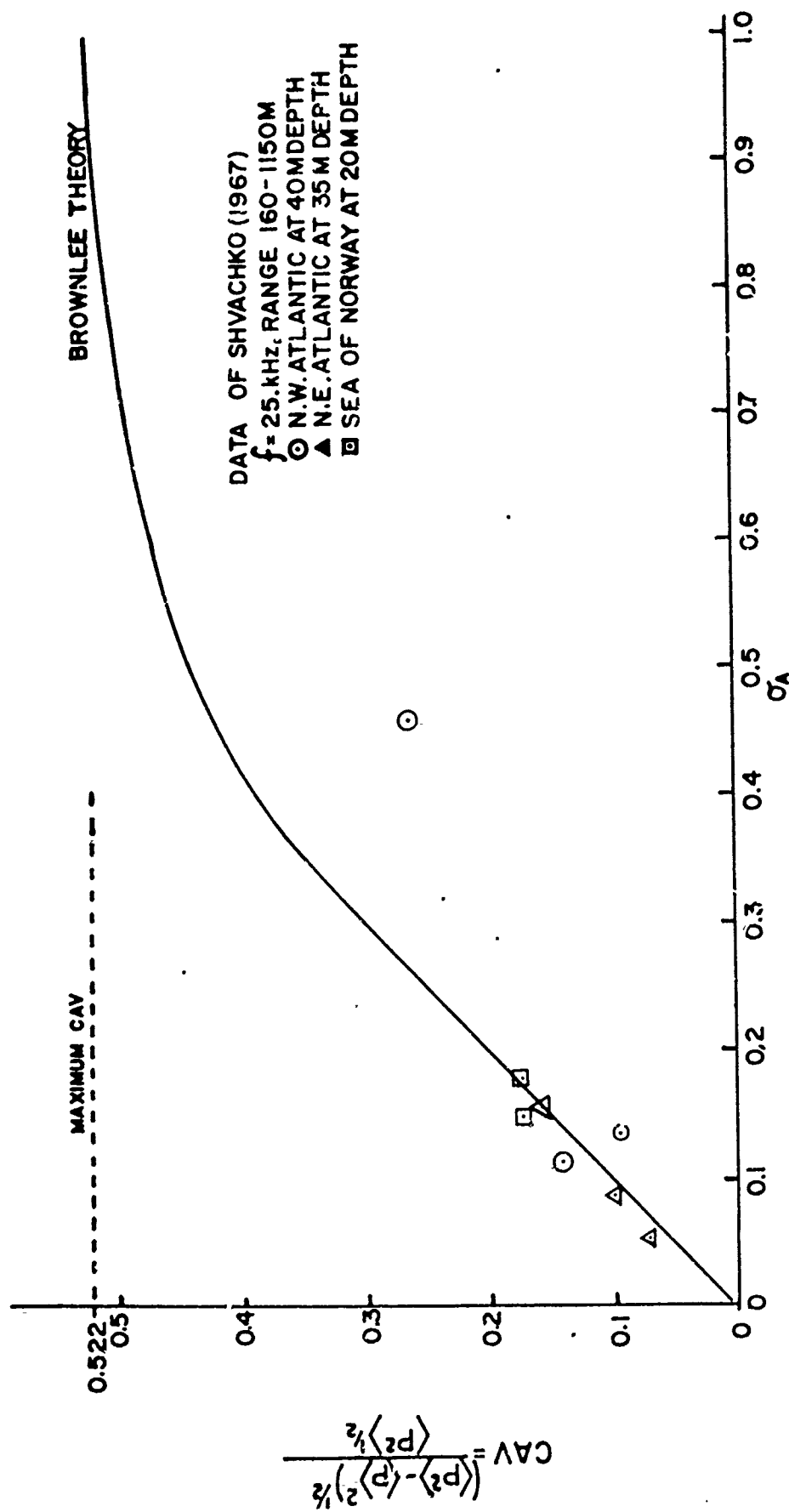


Fig. 8 Coefficient of amplitude variation as a function of the standard deviation of amplitude fluctuations for small fluctuations,  $\sigma_A$ . The data of Shvachko (1967) at 25 kHz are shown. The fluctuations are assumed to be due to microstructure only.

which is the graph of the square root of (3.37). We observe that the fluctuations  $(CAV) = \sigma_A$  for small values of  $\alpha_s R$ , that is, for small fluctuations. The linear dependence of  $(CAV)$  on range continues until approximately  $\sigma_A = 0.35$  after which growth slows.  $(CAV)$  reaches 90% of its ultimate value at approximately  $\sigma_A = 0.6$ .

Knowing the microstructure constants,  $\sigma_\mu^2$  and  $a$ , Fig. 8 and Eq. (3.37) may be used to determine the range at which the CAV due to microstructure can be expected to reach any value up to the maximum  $CAV = 0.522$ .

### 3.5 Sound Fluctuations at Sea

In section 2 we found that the beautiful, and easily manipulated, Gaussian correlation function is precisely correct only for very small spatial lags at sea. In the previous section we saw that the Gaussian correlation function may yield the wrong answers for the coefficient of amplitude variation, even when very carefully tested in the laboratory. It is time to turn to the expression for the limited microstructure correlation function developed in section 2 for an assumed, reasonable, ocean spectrum, Eq. (2.18).

The standard deviation of the phase fluctuations and the coefficient of amplitude variation for all values of the wave parameter, depend on the integration of the spatial correlation function over all values of  $\xi$  from  $\xi = 0$  to infinity. Let us look realistically at the upper limit of the integrations such as in Eq. (3.7) and (3.14) which yield  $\sigma_\phi$  and  $\sigma_A$ . However, although the correlation, defined by

$$C_\mu(\xi) = \frac{\langle \mu(x) \mu(x+\xi) \rangle}{\sigma_\mu^2}$$

can be determined for any spatial lag, the value of  $C_\mu(\xi)$  at  $\xi > R$  is quite irrelevant to a calculation of the sound fluctuations for a path of extent,  $R$ . Therefore practical acoustical application of integrals of  $C_\mu(\xi)d\xi$  will be satisfied by an upper integration limit,  $R$ , rather than  $\infty$ .

The microstructure study of section 2.2 leads us to have confidence in the form of  $C_\mu(\xi)$  only for spatial lags over which the Kolmogorov spectrum is dominant. We have set these limits as  $0 < \xi < \pi/\chi_t$ . In order to evaluate the remainder of the integral consider Fig. 9 which is based on temperature measurements by Seymour (1971) and transformation to spatial coordinates by Haley (1972). The experiment was performed at a depth of 7.3 m, using the stable NUC Oceanographic Tower, 1 mile off San Diego. At this depth, Fig. 3 indicates a microstructure with transition wave number,  $\chi_t \approx 0.075 \text{ cm}^{-1}$ . Equation (2.18) then gives the Kolmogorov-dominated spatial correlation function plotted as the dotted line curve to its expected limit  $\xi = \pi/\chi_t = 42 \text{ cm}$ . The agreement with the experimental data is excellent until  $\xi \approx 25\text{--}30 \text{ cm}$ , after which

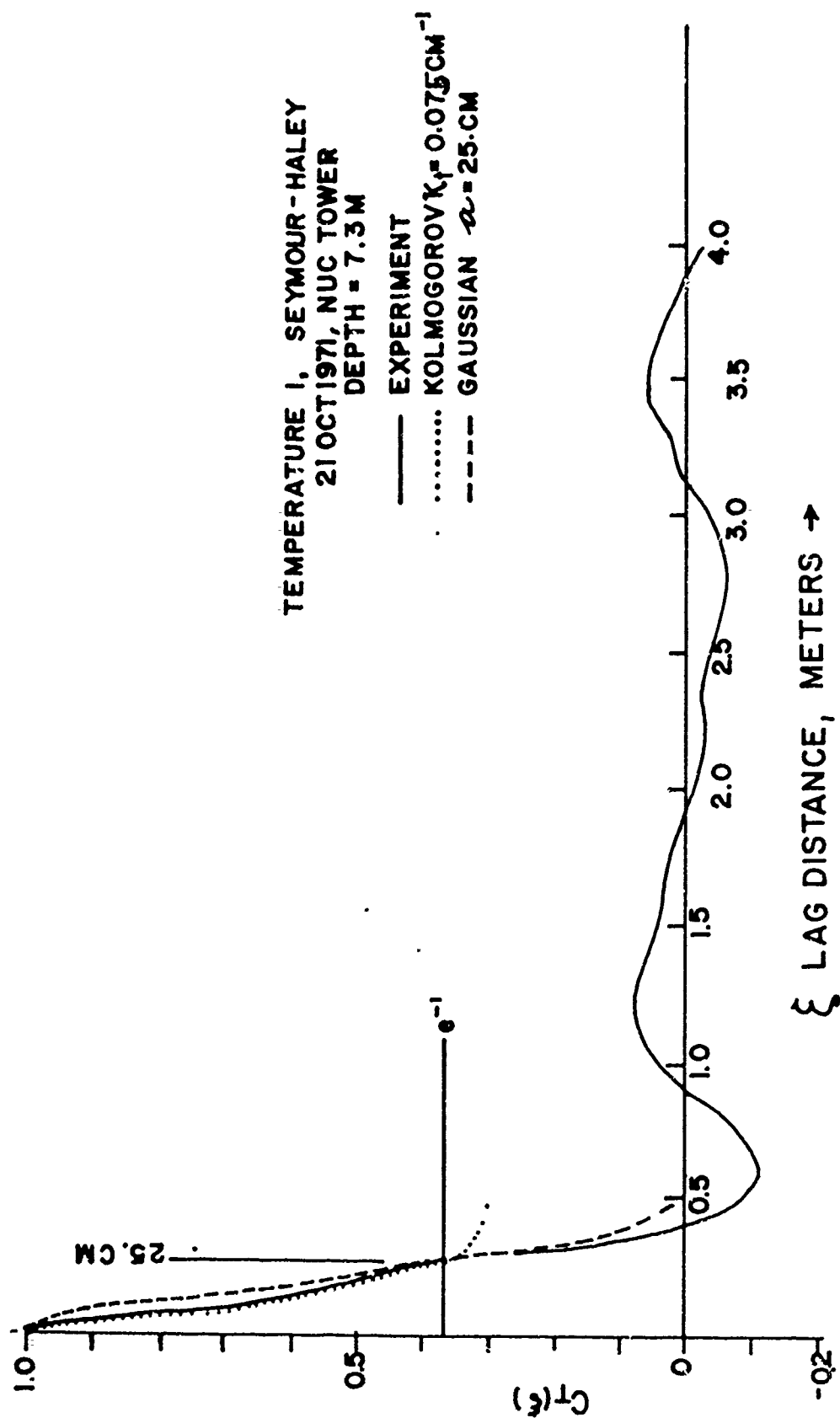


Fig. 9 Spatial correlation function of temperature microstructure at a depth of 7.3m. The solid line is the experimental measurement. The dotted line is the truncated universal correlation function based on the Kolmogorov spectrum from Fig. 6 with  $\kappa_t = 0.075 \text{ cm}^{-1}$ . The dashed line is the Gaussian correlation function with the same correlation length, 25. cm, as the Kolmogorov.

it levels off while the actual correlation function shows a continuing decrease and then an oscillation with small amplitude around the zero correlation axis.

In order to obtain the integral of  $C_{\mu}(\xi)$  for a propagation experiment in such a sea we have two choices: One solution would be to determine  $C_{\mu}(\xi)$  and  $C_{\nu}(\xi)$  out to the range of the acoustic experiment; this would not only be a formidable task but unrealistic for any long range experiment. The second, more expedient, choice is to accept a judicious combination of theory and empiricism. We propose to use the theoretically based microstructure of Fig. 6 to determine the correlation length,  $a$ , and then to use the Gaussian correlation function to approximate the true correlation curve. Judging by Fig. 9, this will result in slightly too large a contribution for  $\int C_{\mu}(\xi)d\xi$  between  $\xi = 0$  and  $\xi = 0.5M$ . We will assume that subsequent positive and negative parts of  $C_{\mu}(\xi)$  will cancel each other and contribute nothing to  $\int C_{\mu}(\xi)d\xi$  from  $\xi = 0.5M$  to  $\xi = R$ . In the example being discussed, the value of the correlation length,  $a = 25$  cm.

Having found a suitable way to determine the equivalent correlation length, all of our algebra for the sound fluctuations due to a Gaussian correlation function is assumed to be applicable, even though the true correlation function is by no means Gaussian.

The general method for the determination of the correlation length is found by referring to Fig. 6. The correlation function is down to  $e^{-1}$  at

$$\kappa_t \xi = \kappa_t a = 1.8 \quad (3.39)$$

therefore for our approximation

$$a = \frac{1.8}{\kappa_t}$$

Furthermore, using the empirical approximation to the transition wave number that we developed from Fig. 3, Eq. (2.8), we have the generalization for the upper ocean.

$$a = 0.2 e^{H/40}$$

$$\text{where } H = \text{depth, m} \quad (3.40)$$

$a$  = temperature (or index) correlation distance in m.

It is evident from the data scatter of Fig. 3, from which the constant  $B$  and  $H$  are determined, that (3.40) can be only a guideline for the prediction of the correlation distance.

Although  $\sigma_\mu$  often decreases with increasing depth, a general rule describing  $\sigma_\mu$  as a function of depth is not possible at this time. In fact, when such a relation is found there will certainly be other important parameters in the equation, such as time of day, to which  $\sigma_\mu$  is particularly sensitive at shallow depths.

When  $\sigma_\mu$  is measured at the place and time of an acoustics experiment, Eq. (3.40) provides a value of correlation length,  $a$ , that completes the needs for evaluating  $\sigma_A$  or  $\sigma_\mu$ . For example, Shvachko (1967) has made measurements of  $\sigma_\mu$  and CAV at depths 20, 35, 40M using sound of frequency 25 kHz. If we take Shvachko's value of  $\sigma_\mu$ ,  $R$ ,  $k$ , and use his depth in Eq. (3.40) to obtain  $a$ , we can calculate  $\sigma_A$  from (3.17) and predict his CAV from (3.37) or the graph Fig. 8. This has been done in the following way:

### ILLUSTRATIVE EXAMPLE

Shvachko (1967) has performed an acoustic fluctuation experiment at frequency 25 kHz, range 20 m, in the sea of Norway. The medium had a standard deviation of the excess index of refraction  $\sigma_\mu = 17.8 \times 10^{-5}$ . We are to calculate the predicted  $\sigma_A$ .

At a depth 20 m reading from Fig. 3  $\kappa_t = 0.055 \text{ cm}^{-1}$  or using (2.8)  $\kappa_t = 9.0e^{-20/40} = 5.45 \text{ m}^{-1}$

therefore from (3.39)  $a = \frac{1.8}{\kappa_t} = 0.33 \text{ m}$

or directly from (3.40)  $a = 0.2 e^{20/40} = 0.33 \text{ m}$

$$k = \frac{\omega}{c} = \frac{2 (25 \times 10^3)}{1.5 \times 10^3} = 104.6 \text{ m}^{-1}$$

$$\text{calculate } D = \frac{4R}{ka^2} = \frac{4(240)}{(104.6)(.33^2)} = 84. \gg 1$$

therefore, using the Gaussian assumption (3.17) for  $D \gg 1$

$$\begin{aligned} \sigma_A^2 &= \frac{\sqrt{\pi}}{2} \sigma_\mu^2 k^2 R a \\ &= (0.89) (17.8 \times 10^{-5})^2 (104.6)^2 (240.) (0.33) \\ &= 0.0244 \end{aligned}$$

$$\sigma_A = 0.16$$

This is to be compared with Shvachko's CAV = 0.17

Since the  $\sigma_A$  is small, we are in the region of the curve (Fig. 8) where we should expect  $CAV = \sigma_A$ . Therefore the small discrepancy between our predicted  $\sigma_A$  and the experimenter's measured value of CAV is a good confirmation of our generalized theory based on the truncated universal correlation function of the temperature microstructure. All of the other data points except one, from the Shvachko experiment, provide similar confirmation as shown in Table 3.1 and Fig. 8.

TABLE 3.1

| Location, Time           | Depth m. | R.m  | $\sigma_\mu \times 10^{15}$ | CAV   | Theory<br>$\sigma_A (\approx CAV)$ |
|--------------------------|----------|------|-----------------------------|-------|------------------------------------|
| N.W. Atlantic, May 1962  | 40       | 200  | 13.7                        | 0.095 | .136                               |
| "                        | 40       | 665  | 25.4                        | 0.264 | .46                                |
| "                        | 40       | 1150 | 4.7                         | 0.141 | .113                               |
| N.E. Atlantic June 1962  | 35       | 940  | 2.7                         | 0.071 | .055                               |
| "                        | 35       | 600  | 5.4                         | 0.100 | .087                               |
| "                        | 35       | 480  | 11.0                        | 0.158 | 0.16                               |
| Sea of Norway, July 1962 | 20       | 160  | 17.8                        | 0.173 | 0.16                               |
| "                        | 20       | 160  | 25.2                        | 0.173 | 0.18                               |

Table 3.1 Comparison of experimental data of Shvachko (1967) with predictions based on the microstructure theory Eq. (3.40 and 3.17) of section 3. Sound frequency, 25 kHz. The points are plotted in Fig. 8 where  $\sigma_A$  is the theoretical value and CAV is the experimental value. The symbols in the first column are those used on the figure.

### 3.6 The Limits of Predictions

The calculation of amplitude fluctuations by the techniques of this report has been constrained by several approximations and assumptions. The ex-post-facto type of comparison with the experiments of Liebermann and Seymour-Haley show that our truncated universal temperature correlation function based on the universality of local microstructure in the upper ocean is not far from the mark, and is usable as a function of depth, alone.

The highly variable values of  $\sigma_\mu$  in the ocean preclude our use of the equations for predicting sound amplitude or phase variations unless we have in-situ data of  $\sigma_\mu$  at the time of the experiment. However, if  $\sigma_\mu$  is available as in the Shvachko experiments, our predictions of  $\sigma_A$  and CAV are quite acceptable.

We have continually emphasized that our predictions are limited to the upper ocean. By this we mean approximately the upper 100 m in temperate or tropical waters. The reason for this restriction is that the recent data of Nasmyth (1972) for depths below 100 m do not fit our Fig. 3 which we use

to determine  $\chi_t$  and correlation distance,  $a$ . The reason is clear, at greater depths in the temperate oceans, and even at shallow depths in the more stable polar regions, the common existence of layers and thin sheets of highly distinctive water masses contradicts our requirement for locally homogeneous, isotropic water. Under these conditions it is not yet possible to generalize in the sense of this section.

A further limitation to our development is the continuing restriction,  $ka \gg 1$ , on which the derivations for  $\sigma_A$  and  $\sigma_\mu$  were based. At shallow depths, say  $H=10$  m, the correlation length is approximately  $a = 30$  cm which constrains the frequency to  $f = \frac{c}{2\pi a} \gg 1$  kHz. At greater depths in the mixed region larger values of  $a$  would relax this limitation. Brownlee (1973) feels that the requirement  $ka \gg 1$  is too strong.

We have not yet considered direction of propagation. Since  $a$  is a function of depth, the fluctuations will vary with angle of inclination of propagation. In principle the solution to the problem can be approximated by integration

$$\sigma_A^2 = \frac{\sqrt{\pi}}{2} k^2 \int_0^R \sigma_\mu^2(z) a(z) dR$$

as in a ray diagram calculation. In practice, although we have equation (3.40) for  $a(z)$

$$a(z) = 0.2e^{z/40} \quad (3.40a)$$

our frustration at generally not knowing how  $\sigma_\mu$  varies with time, or location is now compounded by the non-trivial requirement that  $\sigma_\mu$  be known at all depths along the ray path.

We have also assumed that  $C_\mu(\xi)$  is constant during the time of the experiment. Any inconstancy will, of course, cause a variation in the signal. Some idea of the variation in  $\chi_t$  and  $a$  is possibly indicated by the scatter in data points in Fig. 3.

Throughout this section, the assumption has been made, for simplicity, that  $\sigma_\mu$  and  $C_\mu(\xi)$  are dependent only on the temperature microstructure. In fact, studies of fluctuations of phase have shown that, within approximately 5 to 10 m of the surface (depending on wind speed), fluctuations of the speed of sound and values of  $\sigma_\mu$  are more dependent on variations of bubble radius and number than on temperature fluctuations. This statement is particularly true at sound frequencies near 60 kHz, which corresponds to the resonance frequency of a large population of bubbles. However, for any frequency less than 100 kHz, the complete description of  $\sigma_\mu$  within the upper 10 meters of the ocean will require information about bubbles as well as the temperature structure.

Finally, we must remind the reader that this report deals only with microstructure. To the extent that our study is correct we have evolved a way to understand and to predict the sound fluctuations that are universal, and repeatable. These fluctuations are in fact the minimum fluctuations to be experienced at sea. Any larger scale fluctuations due to internal waves or multipath propagation will be superimposed on the ones that we have studied so far. A fertile field of study remains for the curious. The inverse problem, to predict the  $\sigma_u$  from a knowledge of  $\sigma_\phi$  or  $\sigma_A$  now appears also to be a timely subject for research.

#### 4. Conclusion

A truncated "universal" spatial correlation function of the excess index of refraction has been derived for the upper ocean. The correlation function is predictable from a knowledge of only the depth of the acoustic experiment. Although its applicability is appropriate only for reasonably well-mixed water, and there only for small spatial lags, it appears to be essentially correct to spatial correlations beyond the correlation length, that is, beyond correlation values  $e^{-1}$ . A Gaussian extrapolation of this universal correlation function permits previously derived theoretical expressions for sound phase and amplitude fluctuations to be used without further changes. The predictive technique is simple, and appears to work well for a large range of experimental conditions.



## REFERENCES

- Alexander, C. H. (1974), "Sound Phase and Amplitude Fluctuations in an Anisotropic Medium", M.S. Thesis, Naval Postgraduate School, Monterey, California 93940.
- Batchelor, G. K. (1956), "The Theory of Homogeneous Turbulence", Cambridge University Press, England.
- Batchelor, G. K. (1959), "Small-Scale Variation of Convected Quantities Like Temperature Parts 1 and 2 (with I.D. Howells and A.A. Townsend) in Turbulent Fluid", J. Fluid Mech. 34, 443-448.
- Bergmann, P. G. (1946), Physical Review, 70, 486-492.
- Brownlee, L. R., (1973) "Rytov's Method and Large Fluctuations," J. Acoust. Soc. Am. 53, 156-161.
- Campanella S. J. and A. G. Favret, (1969), "Time Autocorrelation of Sonic Pulses Propagated in a Random Medium", J. Acoust. Soc. Am., 46, 1234-1235.
- Chernov, L. A. (1967), "Wave Propagation in a Random Medium", Dover Pubs., New York, 169 pp. Translated by R. A. Silverman.
- Dunn, D. J., (1965), "Turbulence and Its Effect Upon the Transmission of Sound in Water", J. Sound Vib. 2, 307-327.
- Grant, H. L., A. Moilliet and W. M. Vogel, (1968 a), "The Spectrum of Temperature Fluctuations in Turbulent Flow", J. Fluid Mech. 34, 423-442.
- Grant, H. L., A. Moilliet and W. M. Vogel, (1968 b), "Some Observations Of the Occurrence of Turbulence In and Above the Thermocline", J. Fluid Mech. 34, 443-448.
- Haley, M. C., (1972), "Small Scale Interactions in the Near Surface Ocean", M. S. Thesis, Naval Postgraduate School, Monterey, California 93940.
- Kennedy, R. M., (1969), "Phase and Amplitude Fluctuations in Propagating Through a Layered Ocean", J. Acoust. Soc. Am. 46, 737-745.
- Krasilnikov, V. A., and Obukhov, A. M. (1956), Soviet Physics Acoust., 2, 103-109.
- Liebermann, L., (1951), "The Effect of Temperature Inhomogeneities in the Ocean on the Propagation of Sound", J. Acoust. Soc. Am. 23, 563-570.

- Mintzer, D. , (1953 a and b), "Wave Propagation in a Randomly Inhomogeneous Medium", J. Acoust. Soc. Am. 25, 922-927, II. J. Acoust. Soc. Am., 26, 186-190.
- Nasmyth, P. W., (1970), "Oceanic Turbulence", Ph.D. Thesis, Physics Department, University of British Columbia, (69 pp.).
- Neubert, J. A. and J. L. Lumley, (1970), "Derivation of the Stochastic Helmholtz Equation for Sound Propagation in a Turbulent Fluid", J. Acoust. Soc. Am. 48, 1212-1218.
- Potter, D. S., (1957) and S. R. Murphy, "On Wave Propagation in a Random Inhomogeneous Medium", J. Acoust. Soc. Am. 29, 197-198.
- Sagar, F. H., (1960), "Acoustic Intensity Fluctuations and Temperature Microstructure in the Sea", J. Acoust. Soc. Am., 32, 112-121.
- Seymour, H. A., Jr., (1972), "Statistical Relations Between Salinity, Temperature and Speed of Sound in the Upper Ocean", M. S. Thesis, Naval Postgraduate School, Monterey, California 93940.
- Shvachko, R. F. (1967) "Sound Fluctuations and Random Inhomogeneities in the Ocean", Soviet Physics-Acoustics 13, 93-97.
- Skudrzyk, E. J., (1961), "Thermal Microstructure in the Sea and Its Contribution to Sound Level Fluctuations", Proceedings NATO Symposium, Lecture 12, pp. 199-233. Ed. by V. Albers, Plenum Press.
- Stewart, R. W. and H. L. Grant, (1962), "Determination of the Rate of Dissipation of Turbulent Energy Near the Sea Surface in the Presence of Waves", J. Geophys. Res., 67, 3177-3180.
- Stone, R. G. and D. Mintzer, (1962), "Range Dependence of Acoustic Fluctuations in a Randomly Inhomogeneous Medium", J. Acoust. Soc. Am., 34, 647-653.
- Stone, R. G. and D. Mintzer, (1965), "Transition Regime for Acoustic Fluctuations in a Randomly Inhomogeneous Medium", J. Acoust. Soc. Am., 38, 843-846.
- Tatarski, V. E., (1967), "Wave Propagation in a Turbulent Medium", translated by R. A. Silverman, Dover Pub., New York, (285 pp.).
- Urlick, H. J., (1967), "Principles of Underwater Sound for Engineers", McGraw-Hill, New York.

Weston, D. E., A. A. Horrigan, S. J. L. Thomas and J. Revie, (1969),  
"Studies of Sound Transmission Fluctuations in Shallow Coastal  
Waters", Phil. Trans. of Roy. Soc. Lond. 265, 567-608.

Woods, J. D. and G. G. Fosberry, (1966-1967), "The Structure of the  
Thermocline", Underwater Association of Malta Report,